International
Progress Report

IPR-09-01

Äspö Hard Rock Laboratory

Backfill and Plug test

Hydraulic testing of core drilled boreholes in the ZEDEX drift

Jan-Erik Ludvigson
Rune Nordqvist
Lennart Ekman
Kent Hansson

GEOSIGMA AB

March 1999

Svensk Kärnbränslehantering AB
Swedish Nuclear Fuel
and Waste Management Co

Box 250, SE-101 24 Stockholm
Phone +46 8 459 84 00

Äspö Hard Rock
Laboratory

Report no.	No.
IPR-09-01	F61K
Author	Date
Jan-Erik Ludvigson Rune Nordqvist Lennart Ekman Kent Hansson	March 1999
Checked by	Date
Mansueto Morosini	March 2009
Approved	Date
Anders Sjöland	2009-04-15

Äspö Hard Rock Laboratory

Backfill and Plug test

Hydraulic testing of core drilled boreholes in the ZEDEX drift

Jan-Erik Ludvigson
Rune Nordqvist
Lennart Ekman
Kent Hansson

GEOSIGMA AB

March 1999

Keywords: Hydraulic testing, ZEDEX drift, Backfill and plug test

This report concerns a study which was conducted for SKB. The conclusions and viewpoints presented in the report are those of the author(s) and do not necessarily coincide with those of the client.

Abstract

The present report documents the performance and results of hydraulic testing in selected core boreholes in the Zedex drift. The holes will be used as rock instrumentation boreholes during the Backfill and Plug Test at Äspö HRL. The testing involves both 1 m long boreholes with 56 mm diameter as well as longer boreholes c. 5 m, 8 m and 25 m long with 56 mm or 76 mm diameter. Only single-hole tests were performed.

The tests were carried out as short-time constant head injection tests since all boreholes tested (except one) were non-flowing before tests. The injection phase was followed by a pressure recovery phase. Furthermore, the tests were carried out as single-packer tests. A specially designed test system was used for the tests. The main evaluation of the tests was performed on data from the recovery phase by a new approach based on a non-linear regression technique combined with a flow simulation model (SUTRA).

The tests in the 1 m-holes (testing the interval c. 0.3-0.7 m in the rock perpendicular to the tunnel face) show that the hydraulic conductivity of the superficial rock around the Zedex drift in general is low. However, during testing in some boreholes, visible leakage in the rock occurred through superficial fractures into the tunnel. These fractures were mainly located in the floor of the Zedex drift and are probably blast–induced. These fractures have a high hydraulic conductivity. The tests in the longer boreholes show that the hydraulic conductivity further into the rock in general is below c. $1 \cdot 10^{-10}$ m/s. Increased hydraulic conductivity (c.$1.5 \cdot 10^{-8}$ m/s) was only observed in the flowing borehole KXZSD8HL.

Sammanfattning

Föreliggande rapport dokumenterar utförandet och resultaten av hydraulisk testning i utvalda kärnborrhål i Zedex-orten. Hålen skall användas som registreringshål under Backfill and Plug Test i Äspö HRL. Testningen omfattade både 1m-hål med 56 mm diameter såväl som längre borrhål, c. 5 m, 8 m och 25 m långa med 56 mm eller 76 mm diameter. Bara enhålstester utfördes.

Testerna utfördes som korttids injektionstester med konstant tryck eftersom alla testade borrhål (utom ett) var icke-flödande före testerna. Injektionsfasen följdes av en tryckåterhämtningsfas. Vidare utfördes testerna som enkelmanschett-tester. Ett speciellt utvecklat testsystem användes för testerna. Den huvudsakliga utvärderingen av testerna utfördes på data från återhämtningsfasen med en ny metod baserad på icke-linjär regression kombinerad med en flödesmodell (SUTRA).

Testerna i 1 m-hålen (testar intervallet c:a 0.3-0.7 m i berget vinkelrätt mot tunnel-väggen) visar att den hydrauliska konduktiviteten i det ytliga berget runt Zedex-orten vanligen är c:a $5 \cdot 10^{-10}$ m/s eller lägre. Emellertid, vid testning i några borrhål förekom synligt läckage i berget genom ytliga sprickor in i tunneln. Dessa sprickor var huvudsakligen belägna i sulan av tunneln och är troligen inducerade av sprängningen. Dessa sprickor har hög hydraulisk konduktivitet. Testerna i de längre borrhålen visar att den hydrauliska konduktiviteten längre in i berget vanligen är lägre än c:a $1 \cdot 10^{-10}$ m/s. Förhöjd hydraulisk konduktivitet (c:a $1.5 \cdot 10^{-8}$ m/s) observerades bara i det flödande borrhålet KXZSD8HL.

Executive Summary

The present report documents the performance and results of hydraulic testing in selected core boreholes in the Zedex drift to be used as rock instrumentation boreholes during the Backfill and Plug Test at Äspö HRL. The testing involves both 1 m long boreholes with 56 mm diameter as well as longer boreholes c. 5 m, 8 m and 25 m long with 56 mm or 76 mm diameter. Only single-hole tests were performed.

The tests were carried out as short-time constant head injection tests since all boreholes tested (except one) were non-flowing before tests. The injection phase was followed by a pressure recovery phase. The duration of each phase was 15 min. Furthermore, the tests were carried out as single-packer tests. In the 1 m-boreholes a specially designed mechanical packer of 0.35 m length was designed. In the other boreholes a hydraulic packer of 1 m length. A specially designed test system was used for the tests.

The main evaluation of the tests was performed on data from the recovery phase by a new approach based on a non-linear regression technique combined with a flow model solved by a numerical code (SUTRA). Borehole storage effects, caused by deformation of the components of the test system and water, were considered by the analysis. A steady-state evaluation on data from the injection phase was also made to check the consistency of results from the injection- and recovery phase.

The tests in the 1 m-holes (testing the interval c. 0.3-0.7 m in the rock perpendicular to the tunnel face) show that the hydraulic conductivity of the superficial rock around the Zedex drift in general is c. $5 \cdot 10^{-10}$ m/s or lower. However, during testing in some boreholes, visible leakage in the rock occurred through superficial fractures into the tunnel. These fractures were mainly located in the floor of the Zedex drift and are probably blast–induced. These fractures have a high hydraulic conductivity. If the tests with visible rock leakage are excluded, the geometric mean of the estimated hydraulic conductivities of the other 1 m-holes is $K_{gm} = 2 \cdot 10^{-10}$ m/s.

The tests in the longer boreholes show that the hydraulic conductivity further into the rock in general is below c. $1 \cdot 10^{-10}$ m/s. Increased hydraulic conductivity (c.$1.5 \cdot 10^{-8}$ m/s) was observed in the flowing borehole KXZSD8HL. If this borehole is excluded, the geometric mean of the estimated hydraulic conductivities of the other long boreholes (total length) is $K_{gm} = 3 \cdot 10^{-11}$ m/s. As before, this value is uncertain since several of the tests were below the practical lower measurement limit of the test system

The section of main inflow in KXZSD8HL was localised to 10-14 m by inflow measurements. According to core mapping, borehole radar and TV-camera (BIPS)-measurements a potential water-bearing fracture is located at c. 12.8 m in this borehole. According to BIPS-measurements this fracture has a NW-orientation (strike/dip=147/62) which is in good agreement with the reported dominating orientation of fractures in the A-boreholes around the Zedex drift (139/79). Borehole radar combined with tunnel mapping indicate two NW-fractures with similar orientation and location in KXZSD8HL, intersecting at c. 72 m and c. 69 m length, respectively in the Zedex drift.

Contents

Abstract 3

Sammanfattning 5

Executive Summary 7

Contents 9

List of Figures 11

List of Tables 11

1 Introduction 13

2 Hydraulic tests performed and deviations from the Test Plan 15

3 Test type and strategy 17
3.1 Test type 17
3.2 Test phases 17
3.3 Test strategy 18

4 Test system and performance 19
4.1 Test system 19
4.2 Test performance 20
4.2.1 Injection pressure 20
4.2.2 Effective borehole storage coefficient 20
4.2.3 Packer expanding/inflating pressure 21
4.2.4 Flow rate- and pressure measurements 21
4.2.5 Measurement limits 22

5 Test evaluation 23
5.1 General 23
5.2 Steady-state evaluation of the injection phase 24
5.3 Transient evaluation of the recovery phase 25
5.3.1 Flow simulation model 25
5.3.2 Parameter estimation approach 26
5.3.3 Summary of analysis approach 27

6 Results 29
6.1 Estimated hydraulic conductivity 29
6.2 Comparison of results from injection-and recovery 31
6.3 Inflow measurements in KXZSD8HL 33

7 Conclusions 35

References 37

Appendix 1:1 **General Test Plan.** **39**

Appendix 1:2 **Detailed Test Plan and location of the 1 m-holes.** **40**

Appendix 2. **Calibration chart for flow meter used.** **43**

Appendix 3. **Observed and simulated recovery curves of the tests.** **45**

Appendix 4. **Result tables from the injection- and recovery phases.** **51**

Appendix 5. **Structural model of the Zedex drift including boreholes.** **55**

List of Figures

Figure 4-1 Test system for constant head tests with a mechanical packer in the borehole. 19

Figure 5-1 Observed pressure (p) and flow rate (Q) behaviour in the boreholes during the constant head injection tests. 24

Figure 6-1 Histograms of estimated hydraulic conductivity from the recovery phase (K_R) for the tested 1 m- boreholes at different locations in the Zedex tunnel. 30

Figure 6-2 Histograms of estimated hydraulic conductivity from the recovery phase (K_R) for the tested c. 5 m, 8 m and 25 m-boreholes at different locations in the Zedex tunnel. The intervals above the bars refer to the tested sections. 30

Figure 6-3 Cross-plot of estimated hydraulic conductivity from the recovery phase (K_R) and the injection phase (K_{ss}) for the 1 m-boreholes. Note: Holes with K_{ss} above the upper measurement limit due to rock leakage are not included. 32

Figure 6-4 Cross-plot of estimated hydraulic conductivity from the recovery phase (K_R) and the injection phase (K_{ss}) for the c. 5 m and 8 m-boreholes. 32

List of Tables

Table 3-1 Test phases used for constant head injection tests with different type of single packer. 17

1 Introduction

Single-hole hydraulic tests were carried out in selected rock instrumentation boreholes in the Zedex tunnel prior to the Backfill and Plug Test. The main purposes with the hydraulic tests were to make an initial hydraulic characterisation of selected core boreholes drilled from the Zedex tunnel and investigate their hydraulic communication via eventual fractures in the surrounding rock. In particular, fractures that may act as potential leakage flow paths in the rock during the Backfill and Plug test should be identified and characterised.

2 Hydraulic tests performed and deviations from the Test Plan

The main Test Plan from the Quality Plan of the Project is shown in Appendix 1:1. The hydraulic testing involved new rock instrumentation boreholes (1 m, 5 m and 25 m) as well as old instrumentation boreholes. Subsequently, the selection of which of the 1m-holes to be tested was made by Clay Technology (Appendix 1:2). In this Appendix the location of the 1m-boreholes is also shown. The location of the longer boreholes is shown in Appendix 5.

In the testing campaign, some deviations from the Test Plan in the Quality Plan were made. The deviations are discussed below. The other boreholes were tested according to the Plan. The tests were mainly carried out during September-October 1998. The 5 m-borehole KZ0041G02 was tested in January 1999 since the hole was not accessible during the main testing campaign.

Regarding the 1 m-holes, borehole KZ0052G01 (UR47) was probably (partially) grouted (measured length only 0.1 m) and therefore not tested. During initial testing of some of the 1 m-holes (UR23, UR50-52) it was noticed that gas/water bubbles escaped from one or several fractures in the tunnel face in the vicinity of the tested borehole, indicating local hydraulic communication through superficial fractures close to the tunnel face. Similarly, borehole UR48 is located in intensely fractured rock. No further testing was carried out in these boreholes. The hydraulic conductivity of these boreholes was considered to be above the upper measurement limit of the actual test system used for testing.

Furthermore, it was observed that the hole KXZSD8HR penetrated into the TBM-tunnel. No tests were performed in this borehole. Instead, it was decided to broadly locate the main inflow to the flowing borehole KXZSD8HL (25.98 m long) in the opposite wall.

Finally, no tests could be carried out in the axial boreholes KXZA1, -A2 and –A6 due to time- and economical restrictions and other interfering activities going on in the Zedex tunnel. Identification of potentially water-conductive fractures in boreholes KXZA1, -A2, -A4 and –A5 was previously made by Ludvigson (1997)[1].

Another deviation from the Quality Plan was that the length of the mechanical packer, used for the tests in the 1 m-holes, was changed to 0.35 m (instead of 0.20 m). The latter length was considered too short to effectively isolate the tested sections hydraulically from superficial fractures in the rock close to the borehole at the tunnel face (damaged zone). Since the 1 m-boreholes are inclined 45° the penetration depth in the rock is rather small.

[1] Ludvigson, J-E, 1997: Identification of potentially water conductive fractures in the Zedex-boreholes A1, A2, A4 and A5 and a proposal to packer configurations in the boreholes. Internal pm.

3 Test type and strategy

3.1 Test type

All tests were performed as single-hole tests and furthermore, as single-packer tests. Thus, the tested sections were delimited by a single packer, either at the top of the borehole or at a certain distance in the borehole, and by the bottom of the hole. Since all tested boreholes (except one) were non-flowing, the tests were carried out as injection tests with a constant head with a subsequent recovery period.

Two different types of packers were used. For the tests in the 1m long boreholes (ϕ56 mm) a specially designed mechanical packer of 0.35 m length was used. For the tests in the other boreholes a hydraulic packer of 1 m length was used (both ϕ56 mm and ϕ86 mm boreholes).

In the flowing borehole KXZSD8HL the main inflow was localised by inflating a single packer at certain positions along the hole and measure the flow out of the hole, behind (through a hose) and in front of the packer.

3.2 Test phases

The test phases used for the constant head injection tests are shown in Table 3-1. The packer expanding/inflation time depends on the type of packer used. The duration of the injection- and recovery phases was the same for all tests.

Table 3-1. Test phases used for constant head injection tests with different type of single packer.

Type of packer	Length (m)	Packer exp./infl. (mins)	InjectionPhase (mins)	RecoveryPhase (mins)	Boreholes tested
Mechanical	0.35	15	15	15	1 m holes
Hydraulic	1	30	15	15	other holes

3.3 Test strategy

Firstly, all boreholes were tested with the single-packer located at the top of the borehole close to the tunnel face. To prevent the packer from damage when expanding/inflating, the top of the packer was generally pushed a few centimetres into the hole. Thus, in the 1 m long boreholes the section tested along the hole was 0.43 m - c. 1 m (bottom of hole). Since the boreholes are inclined 45° this length corresponds to a penetration depth interval in the rock of c. 0.3-0.7 m perpendicular to the tunnel face.

Accordingly, in the c. 5 m and c. 8 m long boreholes (with hydraulic packer) the first section tested was generally c. 1.0 m to the bottom of hole or alternatively, 1.5 m to the bottom of hole if the upper part of the hole was very fractured. The (eventual) second single-packer test was performed by pushing the packer 2 m further into the hole and testing the inner part of the hole (if the estimated hydraulic conductivity of the first test was above $1 \cdot 10^{-10}$ m/s). Thus, the second section tested was 3.0 m (or 3.5 m) to the bottom of the hole.

4 Test system and performance

4.1 Test system

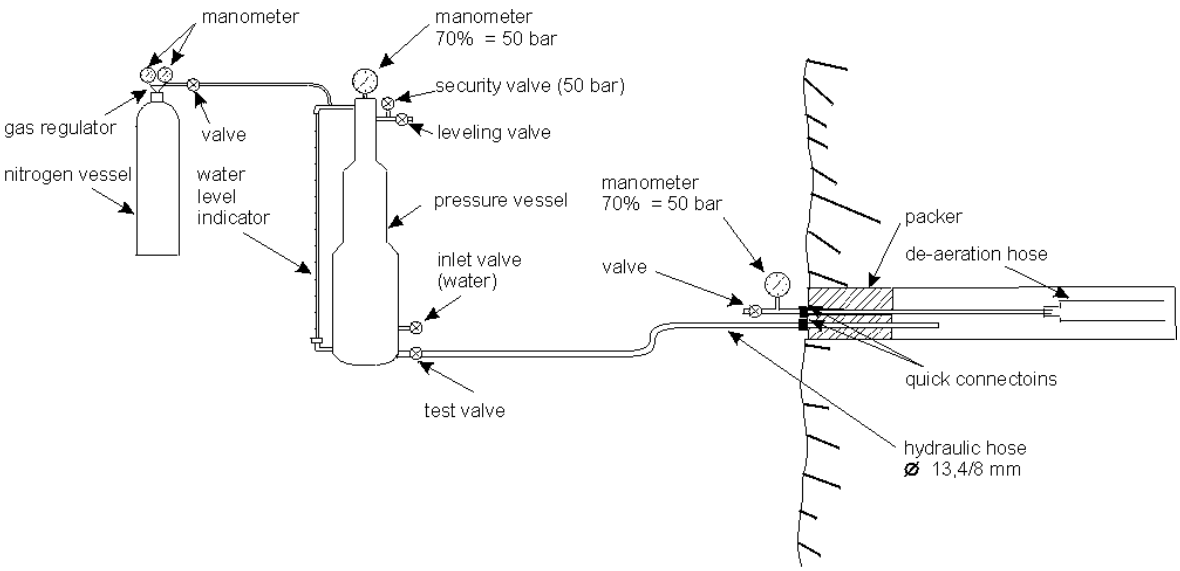

Figure 4-1. *Test system for constant head tests with a mechanical packer in the borehole.*

A specially designed test system was constructed for the tests. In Figure 4-1 the test system used for constant head injection tests with a mechanical packer in the borehole is shown. In principle, the system consists of a pressure vessel (used to measure the injected water volume) with three different diameters to increase the measurement range. On the pressure vessel a graduated standpipe, used to measure the decline of the water level during injection, is mounted. The pressure vessel is connected to a nitrogen gas vessel and -regulator. When a hydraulic packer is used in the borehole an extra nitrogen vessel, gas regulator and pressure vessel together with an extra hose for packer inflation is connected to the system.

Prior to testing the boreholes must be de-aired. In non-flowing boreholes directed upward, water is injected through the lower connection in the packer into the borehole and trapped air is drained through the de-airing hose. In holes directed downward, the hydraulic hose and the de-airing hose are shifted on the packer connections and air is drained through the lower packer connection. During the injection phase, water is injected into the borehole through a reinforced hydraulic hose (∅ 13.4/8 mm) from the pressure vessel by opening the test valve. The recovery phase starts by closing the test valve and the pressure recovery in the test section is measured.

The pressure in the tested section is manually recorded on a large-diameter manometer close to the borehole with a mark for every 1 bar (70 % = 50 bar). The average flow rate (during injection) is measured from the change of water level in the graduated standpipe on the pressure vessel during a certain time period. The calibration curve between water level change and volume injected is shown in Appendix 2. The different slopes of the curve correspond to the different diameters of the pressure vessel.

The test system can also be used for constant drawdown tests in flowing boreholes. Such tests are performed by adjusting the natural flow from the tested borehole section to achieve a constant head (drawdown) during the flow period and then closing the test valve to let the pressure recover in the section. In flowing boreholes, the pressure- and nitrogen gas vessels in Figure 4-1 are not needed during testing. The flow rate may be measured manually by a graduated vessel and stop watch.

4.2 Test performance

4.2.1 Injection pressure

For injection tests, pressure was applied to the tested borehole section by opening the nitrogen gas vessel and the test valve. The pressure was held constant during the injection phase by the gas regulator. The natural background hydrostatic pressure in the rock in the neighbourhood of the Zedex tunnel is in most cases unknown before testing (sufficient time to reach natural pressure stabilisation in the tested section before each test could not be allowed). The applied pressure should exceed the maximal pressure observed in boreholes in the Zedex tunnel (c. 35 bar) to be sure to achieve a certain (positive) injection pressure (dp_s). Therefore, the pressure applied during the injection phase was c. 40 bar.

4.2.2 Effective borehole storage coefficient

During the initial phase of injection, a certain volume of water was rapidly displaced, resulting in a rapid decrease of the water level in the standpipe. This was mainly due to compression of equipment components (hoses, packers, tubes etc.) together with a slight compression of the water volume in the pressure vessel and the tested section. In addition, any trapped air in the test system, e.g. due to insufficient de-airing before the tests, and slight movements of the packer (creeping) during testing will have the same effect.

These effects are similar to conventional borehole storage effects (WBS), commonly appearing in isolated low-conductive sections during the recovery phase of constant head tests due to the compressibility of water and any equipment deformation. Prior to testing, the (effective) borehole storage coefficient of the actual test system was determined in the laboratory from simulated tests.

The initial decrease of the water level in the standpipe (converted to water volume) during the injection phase was used to estimate the actual, effective borehole storage coefficient (C_{eff}) of the test system under field conditions:

$$C_{eff} = \frac{\Delta V}{\Delta p} \qquad (4\text{-}1)$$

where ΔV= initial volume displaced (m^3)

Δp= applied pressure (Pa)

C_{eff} was estimated for each test and compared with the value determined in the laboratory. In most cases reasonable agreement was obtained between values on C_{eff} estimated from the field and laboratory, respectively but in a few cases higher C_{eff}-values were calculated in the field. This may either depend on insufficient de-airing of the system before the test (particularly in boreholes directed upward) or alternatively, slight movements of the packer during testing due to high forces on the packer (anchoring problems).

The latter problem was observed by testing of the 86 mm-boreholes (with hydraulic packers). During these tests, a certain back-flow of displaced water by packer deformation (during injection) was observed when the test valve was opened and the pressure was released after the recovery phase. From this back-flow, which should represent the elastic deformation of the packer, C_{eff} was re-estimated.

For the hydraulic tests performed in the Zedex tunnel the estimated C_{eff} from the injection phase ranged from c. $4 \cdot 10^{-12}$ m^3/Pa to c. $6 \cdot 10^{-11}$ m^3/Pa. The lower extreme value is similar to the values on C_{eff} determined in the laboratory before the tests. On the other hand, values approaching the higher extreme probably indicate small movements of the packer during the tests due to anchoring problems and/or insufficient de-airing of the borehole sections before the tests.

During the recovery phase, C_{eff} may possibly be lower than that estimated from the injection phase, particularly in cases where slight movements of the packer occurred in the beginning of the injection phase. It can be assumed that the packer was more rigid and settled during the recovery phase, e.g due to longer expansion/inflation time elapsed. These facts may lead to that C_{eff}, as calculated as above, in some cases may be overestimated regarding the recovery phase. In cases with apparently high C_{eff}-values due to the above reasons, C_{eff} was reduced by the evaluation of the recovery phase.

From the estimated values on the effective borehole storage coefficient C_{eff}, the corresponding effective compressibility of the test system (c_{eff}) can be calculated according to Eqn. (4-2) for comparisons. In e.g. a 0.5 m section in a 56 mm borehole, the lower extreme value on the borehole storage coefficient shown above ($4 \cdot 10^{-12}$ m^3/Pa) corresponds to an effective compressibility of the entire test system (including water) of $c_{eff}=3 \cdot 10^{-9}$ 1/Pa , c.f. the compressibility of water, $c_w=4.6 \cdot 10^{-10}$ 1/Pa.

$$C_{eff} = V_w \cdot c_{eff} \qquad (4\text{-}2)$$

where V_w = water volume in test section (m^3)

c_{eff} = effective compressibility of test system (1/Pa)

4.2.3 Packer expanding/inflating pressure

The mechanical packer, used in the 1 m long boreholes, was expanded by twisting a screw. The hydraulic packer used in the 56 mm-holes was initially inflated to 45 bar by nitrogen gas. Since this pressure proved to be insufficient in some cases it was increased to 52 bar and occasionally to 55-58 bar. The hydraulic packer used in the 86 mm-holes was inflated to 55 bar. Two rock bolts at each hole anchored the packer.

4.2.4 Flow rate- and pressure measurements

During the injection phase the decline of the water level was recorded manually on the standpipe and converted to volume by the calibration chart. Subsequently, the average flow rates between measurements were determined. The water level (and pressure) was generally measured after c. 5s, 10s, 20s, 40s, 1 min, 2 min, 5 min, 10 min and 15 min after start of injection. The reading precision on the standpipe was c. ±1 mm. The injection phase was terminated by closing the test valve. Then the pressure recovery in the tested section was monitored manually on the manometer according to the same schedule as shown above. The reading accuracy of pressure on the manometer was c.± 0.1 bar.

4.2.5 Measurement limits

For the tests in the 1 m-boreholes with mechanical packer the lower measurement limit of flow rate was in this case estimated to Q_{min}= 0.4 ml/min ($6.7 \cdot 10^{-9}$ m^3/s), considering the uncertainty of the flow rate measurement (reading) and elastic deformation of (mainly) the packer. During the injection phase variations of the pressure (not perfectly constant) also affect the lower measurement limit. The potential error associated with the above estimate of Q_{min} is estimated to c. ±50 %. Assuming an injection pressure of 150 m (see below) this corresponds to a lower measurement limit in terms of transmissivity of $T_{min}=5 \cdot 10^{-11}$ m^2/s. In e.g. a 0.5 m long section $K_{min}=1 \cdot 10^{-10}$ m/s, c.f. 1m boreholes.

For the hydraulic packers, the following estimations of the lower measurement limit during the injection phase are based on laboratory measurements on the deformation of different equipment components for tests in the Zedex project[2]. For the actual tests the lower measurement limit of flow rate is estimated to Q_{min}= 1.5 ml/min (with a potential error of c. ±50 %). Assuming an injection pressure of 150 m as above, the lower measurement limit for transmissivity during the injection phase is in this case $T_{min}=2 \cdot 10^{-10}$ m^2/s. In a 2 m long section, $K_{min}=1 \cdot 10^{-10}$ m/s, c.f. the 5 m-holes.

Flow rate, with associated uncertainties, is not measured during the recovery phase (and not implicitly involved in the estimation of the hydraulic parameters from this phase, see Section 5.3). Thus, the lower measurement limit during the recovery phase will mainly depend on the deformation of the packer and not on flow rate. Therefore, this limit may possibly be lower for the recovery phase than that during the injection phase. However, packer deformation probably has the dominating influence in this case and may thus in practice determine this limit for the recovery phase.

The upper measurement limit for the actual test system is rather subjective. The maximal flow rate during injection may correspond to the maximal change of water level in the standpipe (total range) of c. 1400 mm (corresponding to a volume of c. 1370 ml, see Appendix 2) during a certain time, say 4 minutes. These values correspond to an average flow rate of c. $6 \cdot 10^{-6}$ m^3/s (0.36 l/min) during this time interval.

For an assumed injection pressure of dp_s=150 m as above, the upper measurement limit in terms of (steady-state) transmissivity from the injection phase may then be estimated to $T_{max}= 5 \cdot 10^{-8}$ m^2/s. This value corresponds to $K_{max}= 1 \cdot 10^{-7}$ m/s for a 0.5 m section and $K_{max}= 2.5 \cdot 10^{-8}$ m/s for a 2 m section. However, the performance of the actual test system in this measurement range is uncertain. For example, a pressure transducer must probably register the pressure in the tested section, particularly during the recovery phase, to achieve sufficient resolution and accuracy of the test data.

---

[2] Hansson, K., 1994: Preparations for hydrotests in Zedex och TBM-pilot holes – Equipment- and functioning tests in borehole KA2598A together with recommended measuring routines. (In Swedish). Internal report GRAP 94088, GEOSIGMA AB, Uppsala.

5 Test evaluation

5.1 General

The observed variation of pressure and flow rate during the injection- and recovery period of the constant head injection tests are shown in Figure 5-1. All tested boreholes were apparently dry before testing (possibly drained by the tunnel). Thus, the starting pressure (P_0) in the boreholes was zero before testing. However, a short distance into the rock from the borehole face the pressure might be much higher, possibly approaching the natural hydrostatic (environmental) pressure (P_s) in the rock close to the Zedex tunnel. The maximal pressure that previously has been measured in boreholes drilled from the Zedex tunnel is c. 35 bar. The presumed average hydrostatic pressure is likely to be less than this value due to the fact that the boreholes in the Zedex-tunnel might have partially drained the actual rock volume.

Theoretically, the actual shut-in pressure in the boreholes would build up close to the average hydrostatic pressure if sufficient time were allowed for pressure build-up before the tests. Unfortunately, this may take very long times, particularly in low-conductive sections, and was therefore not possible in this case. By the evaluation of the tests, described below, the average hydrostatic pressure in the rock volume around the Zedex tunnel (P_s in Figure 5-1) was assumed to c. 25 bar (250 m).

Since the average hydrostatic pressure is unknown, it means that the actual injection pressure applied to the rock (dP_s) is also unknown. During the recovery phase the pressure in the boreholes will approach, and eventually reach, the average hydrostatic pressure if the hydraulic conductivity is high enough. If, on the other hand, the hydraulic conductivity in the borehole is very low the pressure recovery will be very slow, c.f. Appendix 3.

The main evaluation of the tests was made on data from the recovery phase. A simple steady-state evaluation was also made on the injection phase to check for consistency of the results from the two phases.

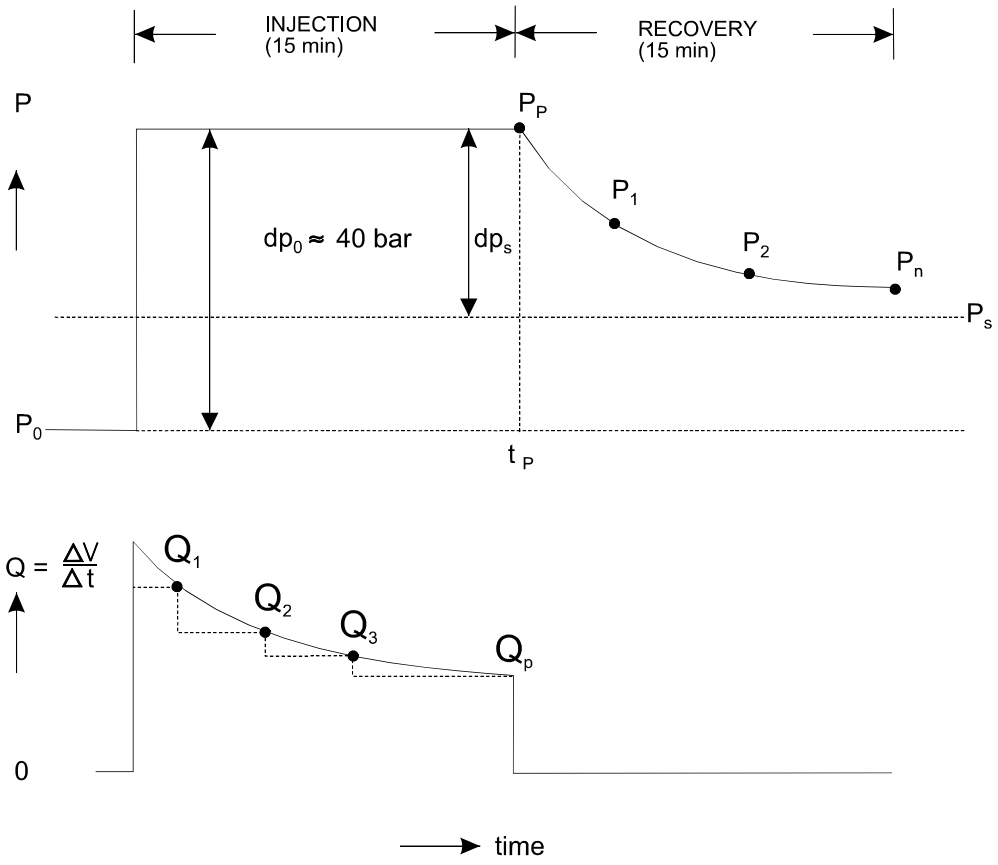

Figure 5-1. *Observed pressure (p) and flow rate (Q) behaviour in the boreholes during the constant head injection tests.*

5.2 Steady-state evaluation of the injection phase

A simple steady-state evaluation was made on the injection phase using Moye's formula:

$$T_{ss} = \frac{Q_p}{dp_s} \times C \tag{5-1}$$

$$C = \frac{1 + \ln(L/d)}{2\pi} \tag{5-2}$$

$$K_{ss} = T_{ss} / L \tag{5-3}$$

T_{ss} = steady-state transmissivity (m^2/s)

K_{ss} = (equivalent porous-medium) hydraulic conductivity (m/s)

Q_p= average flow rate between 10-15 min of injection (m^3/s)

$dp_s = P_p - P_s$ = actual injection pressure (m)

P_p = applied pressure (m)

P_s = natural hydrostatic pressure (assumed to 250 m)

L = section length (m)

d = borehole diameter

Since the applied pressure P_p during injection was c. 40 bar (400 m) and the natural hydrostatic pressure was assumed to c. 250 m, the actual injection pressure dp_s used was c. 150 m in this case. The above equations show that the estimated hydraulic conductivity from the injection phase K_{ss} is inversely proportional to dp_s. Effects of borehole storage are not considered by the evaluation of the injection phase.

5.3 Transient evaluation of the recovery phase

5.3.1 Flow simulation model

The flow simulation model that was used to interpret the hydraulic conductivity from the recovery phase has the following general features:

- Radial flow
- Transient flow
- Borehole storage effects are simulated
- Heads were computed numerically
- Outer constant head boundary located ”far away” approximating an infinite boundary

The flow simulation was generally carried out in the following three steps:

1. A steady state simulation of heads, with the purpose of allowing simulation of a drawdown cone around the tested section prior to the injection phase. Because most of the tested sections were ”dry”, i.e. drained by the tunnel prior to the tests, prior drawdown was assumed in most cases. Boundary conditions are constant head in both the tested borehole section and at the outer boundary.

2. A transient simulation of the injection phase, with the results from step one (steady-state drawdown) as initial conditions. Boundary conditions are constant head in both the borehole section and at the outer boundary.

3. A transient simulation of the recovery phase using the results from step 2 as initial conditions. Boundary condition is constant head at the outer boundary, but no boundary condition (i.e. no flow) at the borehole boundary.

The reason for using such a relatively elaborate simulation strategy is that the hydraulic conditions prior to this type of test may have a significant effect on the recovery curve, and thereby also estimation of hydraulic parameters from it. If a drawdown cone prior to the test exists around the tested section, the ”background” head distribution may be more or less unknown. Thus, if recovery is measured during only a short period, the head value that the recovery approaches is unknown. In addition, a short-duration injection period results in far from steady state conditions prior to recovery. These are the reasons for considering the entire hydraulic ”history” in the simulation model, aside from the consideration that it is conceptually more appealing in general.

Borehole storage effects are included in the simulation model because these may affect the recovery curve significantly. In fact, in low-permeability sections the entire recovery curve (for short-duration tests such as this) may be significantly influenced by borehole storage.

The simulation model was implemented by using subroutines from the SUTRA code (Voss, 1990). SUTRA is a finite element code for simulation of flow and transport in two dimensions. SUTRA was considered a good choice for this type of analysis since it is widely used, well documented and computationally robust. In fact, it may be argued that a well-tested numerical solution method may be advantageous compared to an analytical one. A numerical method (such as finite difference or finite element) may be both faster and more accurate (over a wide range of parameter values) than an analytical solution.

Limitations to this model approach include the assumption of radial flow, and the assumption of a large distance to the outer boundary (it may be located considerably closer, for example due to the tunnel). However, because of the low hydraulic conductivity in most of the tested borehole sections, the outer boundary had no significant influence in most of the simulations. Further, the rock in the vicinity of sections that are completely drained (dry) prior to testing may experience some two-phase flow effects. Borehole skin effects are not considered, but such effects, if significant, are considered to be effectively lumped together with the formation storativity. In spite of the listed limitations, it is argued, because of the consideration of the entire transient head history and borehole storage effects, that this approach has fewer limitations than commonly applied ”standard” methods.

5.3.2 Parameter estimation approach

Non-linear least squares regression (see for example Draper and Smith, 1981) was used to estimate parameters from the recovery phase in the simulation model described in the previous section. The regression was carried with the so called Marquardt method, which may be described as a compromise between gradient search and a Newton-type search method. The software used was PAREST[3], where the simulation model was constructed using subroutines from the SUTRA code.

An advantage with using non-linear regression is that estimation errors are obtained for the estimated parameters, as well as correlations between parameters. This gives a somewhat objective measure of the uncertainty in the regression estimates, i.e. a standard error for each estimated parameter value (for example Cooley, 1987).

[3] Nordqvist, R., 1994: PAREST: a Fortran code for inverse modeling with an arbitrary model using non-linear least squares regression - users manual. Internal report GRAP 94005. GEOSIGMA AB.

The estimation errors are contained in the variance-covariance matrix (using the best-fit estimates):

$$s^2(\mathbf{X}^T\mathbf{X})^{-1} \qquad (5\text{-}4)$$

where **X** is a matrix of parameter sensitivities, and s^2 is the common error variance . The standard errors are obtained from the diagonals in the variance-covariance matrix and the correlations may be calculated from the off-diagonals.

The parameters that were estimated were generally log T_R (transmissivity) and log S' (apparent storage coefficient). The equivalent porous medium hydraulic conductivity K_R from the recovery phase was estimated in analogy with Eqn. (5-3). In some cases, the head value at the outer boundary was also estimated. The borehole storage coefficient was considered known, because it was independently estimated from the initial period of the injection phase, see Section 4.2.2. In addition, the total sum of squares and the standard error SE of each estimation parameter together with the correlation between the parameters were calculated.

5.3.3 Summary of analysis approach

Given below is an outline of the analysis procedure:

1. Input all known variables and parameter values:

- head at outer boundary (250 m in most cases)
- distance to outer boundary (10^4 x borehole diameter in all cases)
- head in borehole prior to injection (generally 0 m)
- duration of injection phase (15 min in all cases)
- constant head during injection phase
- borehole storage coefficient

2. Make initial estimates of estimation parameters.

3. Provide measurement data file from recovery phase.

4. Run PAREST

Plot best-fit solution (compare measured and estimated heads) and examine regression statistics (squared sum of errors, standard errors, and correlations between parameters). The measured recovery data together with the best-fit solutions are shown in Appendix 3 for all tests. On the vertical scale of the diagrams the head values are plotted with maximal resolution. The time axes start at the beginning of the recovery phase.

6 Results

6.1 Estimated hydraulic conductivity

The results and relevant test data from the injection- and recovery phases of the tests in the 1-m-boreholes are presented in Appendix 4 in Tables A4.1a-b,. respectively. The results from the remainder of the tested boreholes are shown in Tables A4.2a-b in this appendix. From the injection phase, the average flow rate Q_p (between 10-15 min) and the applied pressure P_p are shown together with the estimated steady-state transmissivity T_{ss} and (equivalent) hydraulic conductivity K_{ss} are shown. From the evaluation of the recovery phase by non-linear regression the estimation parameter (log T_R) and the associated standard error (SE_{logTR}) together with the transmissivity T_R and (equivalent) hydraulic conductivity K_R are included.

In Figure 6-1 a histogram of the estimated hydraulic conductivity from the recovery phase (K_R) of the tested 1 m-boreholes is shown. The holes are grouped according to their location in the tunnel. The estimated upper and lower measurement limits of the test system used are also indicated. In holes KZ0061B01, -0050G01, -46G01, -43G01 and -41G01 no complete tests could be carried out due to intense fracturing and visible rock leakage through superficial (probably blast induced) fractures during testing. The hydraulic conductivity of these boreholes was considered to be above the upper measurement limit of the test system used. Also in hole –48G01 visible (slight) rock leakage was observed during testing. Hole KZ0052G01 is probably (partially) grouted and was not tested.

The results from the 1 m-holes in Figure 6-1 indicate that the (equivalent) hydraulic conductivity of the rock generally is below c. $1 \cdot 10^{-9}$ m/s (except the holes above or close to the upper measurement limit). If the tests with rock leakage are excluded, the geometric mean of the estimated hydraulic conductivity of the other 1 m-holes is $K_{gm} = 2 \cdot 10^{-10}$ m/s. This value is uncertain since several of the tests were below the practical lower measurement limit of the test system, see Section 4.2.5. The results from the roof and both walls of the tunnel are generally similar whereas the floor shows an increased hydraulic conductivity. The estimated values represent the test section 0.43 m to c. 1 m along the (inclined) boreholes, corresponding to an interval of c.0.3-0.7 m into the rock perpendicular to the tunnel face. Thus, the sections are located in the damaged zone around the tunnel.

In Figure 6-2 a histogram of the estimated hydraulic conductivity from the recovery phase (K_R) of the tested c. 5 m (light blue colour) and the c. 8 m-boreholes (green) is shown. In addition, the estimated hydraulic conductivity of the c. 25 m-hole KXZSD8HL (red) from the inflow measurement is included. The c. 25 m-hole KXZSD8HR was not tested, see Chapter 2. The tested sections are also shown in Figure 6-2. In borehole KXZSD8HL the interval shown corresponds to the section of maximal inflow.

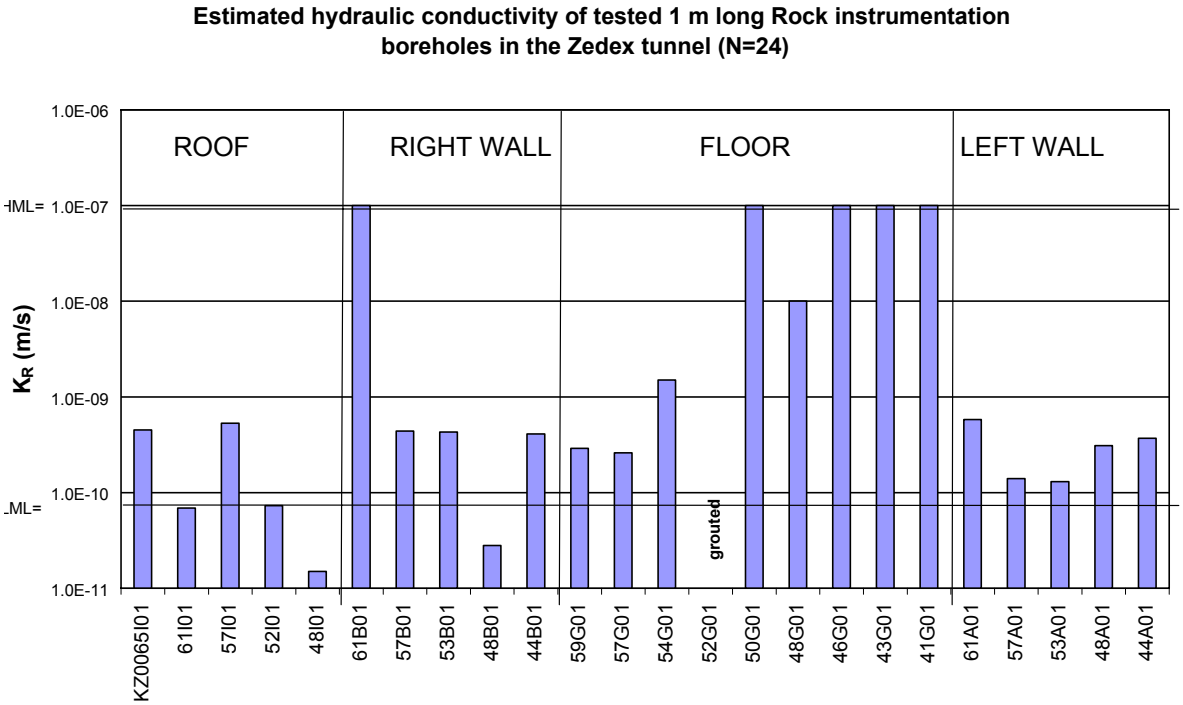

Figure 6-1. *Histograms of estimated hydraulic conductivity from the recovery phase (K_R) for the tested 1 m- boreholes at different locations in the Zedex tunnel.*

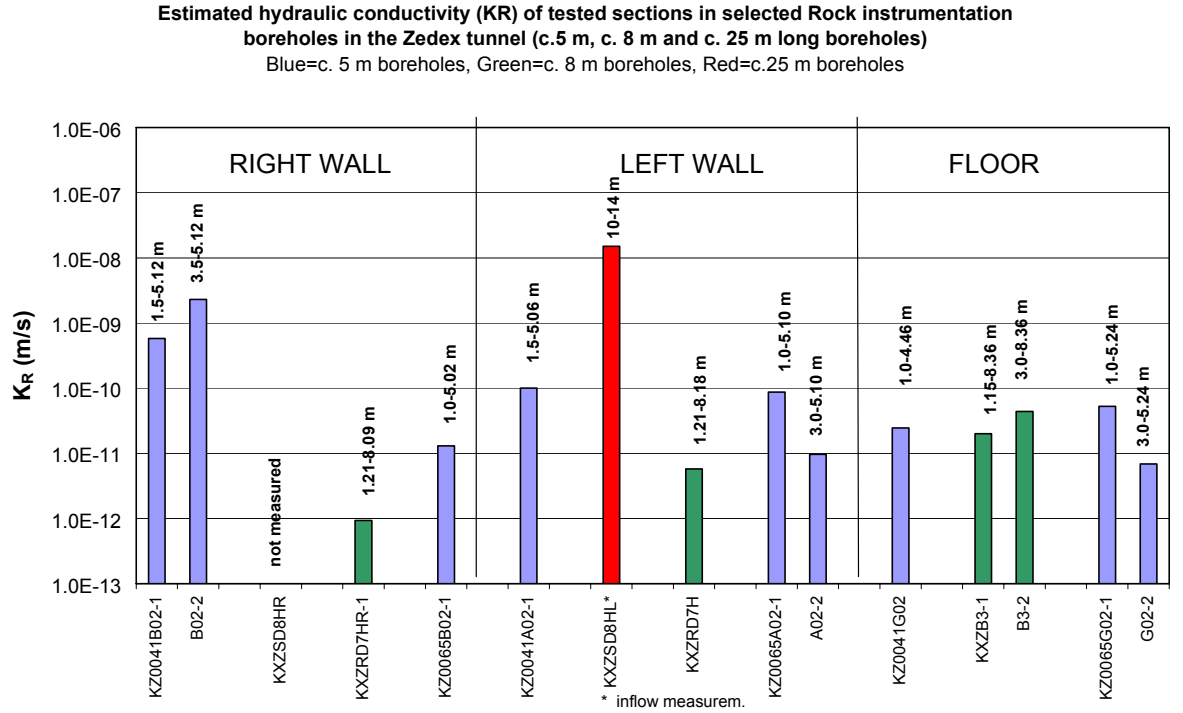

Figure 6-2. *Histograms of estimated hydraulic conductivity from the recovery phase (K_R) for the tested c. 5 m, 8 m and 25 m-boreholes at different locations in the Zedex tunnel. The intervals above the bars refer to the tested sections.*

Figure 6-2 shows that the (equivalent) hydraulic conductivity of the rock some distance from the tunnel face in general is below c. $1 \cdot 10^{-10}$ m/s (except from holes KZ0041B02 and KXZSD8HL). In very low-conductive sections, showing very slow recovery, the estimated hydraulic conductivity must be regarded as very uncertain, independent of interpretation method used. Such sections show high standard errors SE (non-unique results) from the evaluation of the recovery phase in all tests, see Tables A4.1b and 2b in Appendix 4. If KXZSD8HL is excluded the geometric mean of the estimated hydraulic conductivity of the other long boreholes (total length) is $K_{gm} = 3 \cdot 10^{-11}$ m/s. This value is uncertain since several of the tests were below the practical lower measurement limit of the test system, see Section 4.2.5.

The evaluation procedure involving non-linear least square regression, and the transient simulation model, generally worked very well. Best-fit parameter estimates were usually obtained after only a few (typically five or six) iterations, and estimation errors were then also relatively low for both log T_R and log S'. Exceptions to this occurred in tested sections with very low hydraulic conductivity, where only very small changes in head during the recovery phase were measured. In those cases estimation errors were considerably higher, and often of the same magnitude as the estimated values themselves.

In some cases additional parameters were estimated. The borehole storage coefficient was estimated in cases where the prior estimation of it was considered more uncertain, and where the fit between measured and simulated heads showed some systematic errors. However, because of high correlation between parameters (parameter correlations are obtained from the regression) estimation errors (standard errors) were generally unacceptably high when the borehole storage parameters was included. In a couple cases the outer boundary condition (the head at the outer boundary) was estimated, in sections with high permeability and systematic errors in the best-fit solution. In these cases, estimation was improved considerably, and there was generally not a problem to estimate the boundary head along with log T and log S'.

For all of the recovery phases analysed with the transient simulation model and regression, very good agreements between measured data and best-fit simulations were obtained. No significant systematic errors were observed in the fitted recovery curves, see Appendix 3, which implies that the applied simulation model is plausible.

6.2 Comparison of results from injection-and recovery

Figures 6-3 and 6-4, show cross-plots of the estimated hydraulic conductivity from the recovery phase (K_R) and injection phase (K_{ss}) for the 1-m boreholes and the other tested borehole sections, respectively. It should be observed that the evaluation from the injection phase is approximate and was mainly made to check the consistency between the results from the injection- and recovery phases. The main evaluation was performed on data from the recovery phase. Thus, the results from the latter phase are considered to be more accurate. In Figure 6-3, the 1m-boreholes considered to be above the upper

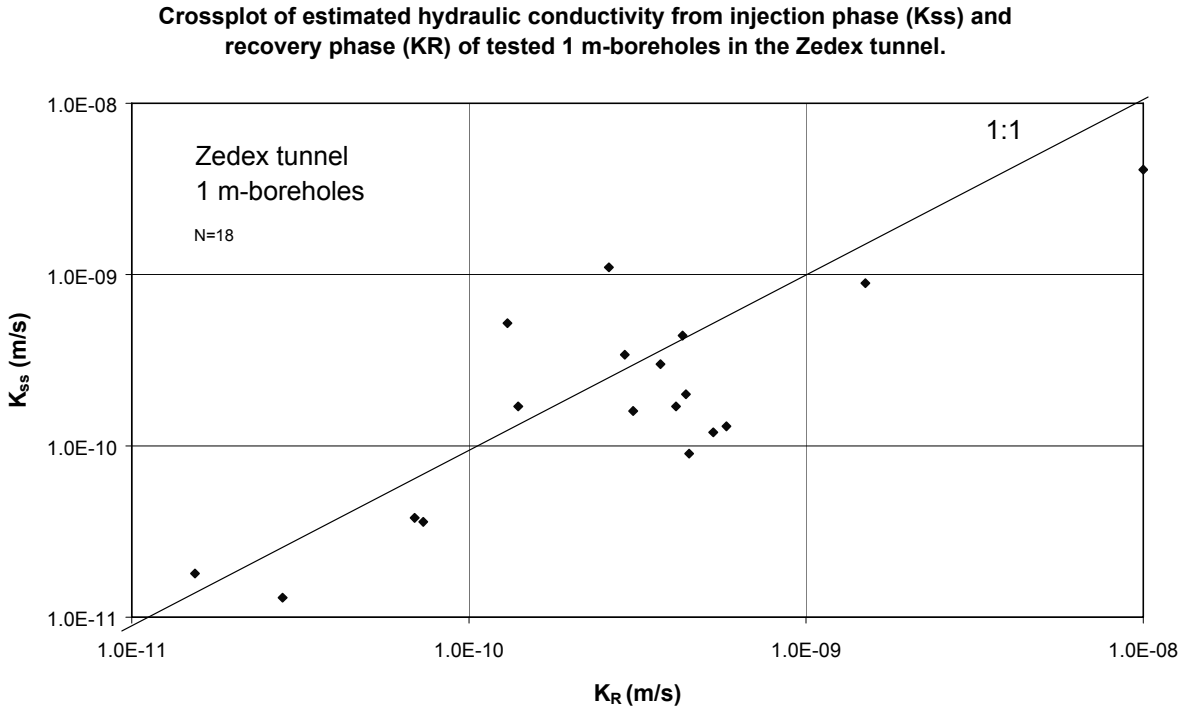

Figure 6-3. *Cross-plot of estimated hydraulic conductivity from the recovery phase (K_R) and the injection phase (K_{ss}) for the 1 m-boreholes. Note: Holes with K_{ss} above the upper measurement limit due to rock leakage are not included.*

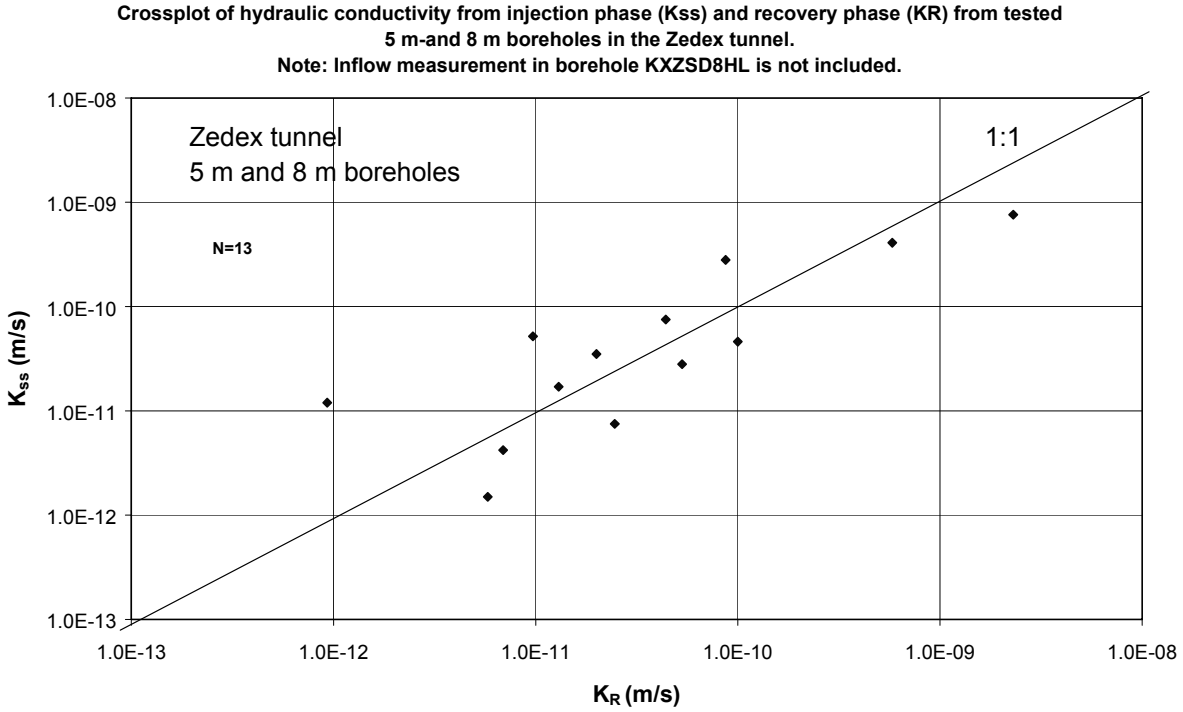

Figure 6-4. *Cross-plot of estimated hydraulic conductivity from the recovery phase (KR) and the injection phase (Kss) for the c. 5 m and 8 m-boreholes.*

measurement limit of the test system are excluded. Furthermore, in Figure 6-4 the result from the inflow measurements is excluded. Figures 6-3and -4 indicate that the agreement between the results from the two (rather independent, see below) test phases in general is good, considering the short-time and simple test method used.

As discussed above, the estimates of the lower measurement limit may differ between the injection- and the recovery phase, see Section 4.2.5. Apart from equipment related factors there are also major differences in the evaluation of test data from the two phases. The data from the injection phase are evaluated by a simple steady-state formula, in which the estimate of hydraulic conductivity mainly depends on the measured flow rate with associated errors and the assumed injection pressure.

Furthermore, the evaluation of the recovery phase is based on regression analysis on data from this phase. In addition, this process also involves simultaneous numerical calculations of both the preceding injection phase and the head distribution before this phase, see Section 5.3. Thus, estimates of the hydraulic conductivity from the recovery phase do not implicitly require input values on neither the flow rate nor the injection pressure (with associated uncertainties) but are calculated by the flow model. This means that the lower measurement limit from the recovery phase is more governed by constraints of certain equipment components, e.g. packers, than by the actual evaluation procedure which has no such limitations.

Another potential difference between the results from the injection- and recovery phase is the consequences of the assumption made of the average, environmental hydrostatic pressure (p_s= 250 m) in the rock close to the Zedex tunnel. The conductivity estimates from the injection phase according to Eqns (5.1-3) are affected in a direct way by this assumption while the estimates from the recovery phase are only affected indirectly (or not affected at all). Since most of the tested sections were low-conductive, the radius of influence of the tests was quite small. In the regression analyses of the recovery phase the assumed hydrostatic pressure of 250 m corresponds to a distant boundary condition ($r_e=10^4 \cdot d_w$), see Section 5.3. Thus, this condition has little or no influence on the evaluation of the recovery data.

Finally, borehole storage effects, discussed in Section 4.2.2, including deformation of equipment, small movements of the packer during testing and any trapped air in the system are not considered by the evaluation of the injection phase but are considered by the recovery phase. Errors in the estimation of C_{eff} may thus affect the latter evaluation, in particular when high values on C_{eff} were calculated from the injection phase.

6.3 Inflow measurements in KXZSD8HL

The main inflow of water (c. 0.9 l/min) in borehole KXZSD8HL was localised to section 10-14 m. This inflow corresponds to a hydraulic conductivity of this section in the order of $K_{ss}= 1.5 \cdot 10^{-8}$ m/s with the same assumption of environmental head as before (250 m).

From BIPS-measurements (borehole TV inspection) in KXZSD8HL two potential water-conducting fractures at c. 10 m and 12.8 m , respectively were interpreted in the interval 10-14 m (Stråhle 1998, pers. comm.) The first one intersects narrow greenstone and aplite veins. Both the aplite vein and the fracture have a NE strike but the vein has a steep dip

and the fracture a shallow dip. The fracture is partly open. The second fracture at 12.8 m is open and has a NW strike with a sub-vertical dip (147/62). This fracture has also been identified from core mapping and borehole radar measurements (Carlsten 1998). The extrapolation of the latter fracture, as interpreted from the BIPS-survey, is shown in Appendix 5.

In Appendix 5, the previous structural characterisation of the Zedex drift (Stenberg and Gunnarsson 1998), including observed water-bearing fractures in tunnels and boreholes (blue colour) and possible interconnections in the rock between these fractures are shown. All interpreted water-bearing structures have a NW-orientation, which may indicate that the extrapolated NE-fracture, described above, is less conductive.

On the other hand, the orientation of the interpreted NW-fracture is in good agreement with the dominating orientation (139/79) of fractures in the A-boreholes (A1-A7) around the Zedex tunnel according to Stenberg and Gunnarsson (1998). The observed water-bearing NW-fracture at 12.8 m in KXZSD8HL may possibly correlate with the NW-striking fractures intersecting the Zedex tunnel at c. 72 m and c. 69 m, indicated by borehole radar measurements in KXZSD8HL by Carlsten (1998) combined with geological tunnel mapping. The latter two fractures have slightly different strikes and dips than the BIPS-interpreted fracture (302/90 and 318/80, respectively).

7 Conclusions

A new test system for short-time, single-packer constant-head tests with a subsequent recovery period was developed and used in core boreholes in the Zedex tunnel. In addition, a new evaluation method based on non-linear regression of data from the recovery phase was used. Both the new test system and the new evaluation method proved to be successful in the actual measurement range of hydraulic conductivity of the rock surrounding the Zedex tunnel.

In some cases, problems with the anchoring of the packer occurred due to the high pressures applied (40 bar). In addition, the de-airing of the boreholes (particularly in holes directed upward) was probably incomplete in some cases. These problems resulted in an increase of the estimated borehole storage coefficient of the test system for such tests. Borehole storage effects were considered by the evaluation of the recovery phase of the tests.

Consistent hydraulic conductivities were generally obtained from the (rather independent) injection- and recovery phases of the tests although the results from the latter phase are considered to be more accurate.

The tests in the 1m-boreholes show that the hydraulic conductivity of the rock around the Zedex tunnel generally is low. The tested intervals in these holes were 0.3-0.7 m in the rock, perpendicular to the tunnel face. However, during testing in some of the 1 m-holes, visible rock leakage occurred through superficial, probably blast induced fractures in the vicinity of the tested boreholes, generally located in the tunnel floor. The hydraulic conductivity of these boreholes was high, above the practical upper measurement limit of the actual test system used (K_{max}= c. $1 \cdot 10^{-7}$ m/s).

The median value of the estimated hydraulic conductivities of all 1 m-boreholes tested (N=23) is $4 \cdot 10^{-10}$ m/s. The median hydraulic conductivity of the 1 m-holes in the roof (N=5) and walls (N=10) are $7 \cdot 10^{-11}$ m/s and $4 \cdot 10^{-10}$ m/s, respectively. In the tunnel floor, 4 holes out of totally 8 tested holes have hydraulic conductivities above the upper measurement limit. If the tests showing visible rock leakage are excluded, the geometric mean of the estimated hydraulic conductivities of the remaining 1 m-holes is $K_{gm}= 2 \cdot 10^{-10}$ m/s (N=17). This value is uncertain since several of the tests had conductivities below the practical lower measurement limit of the test system (K_{min}= c. $1 \cdot 10^{-10}$ m/s).

The tests in the longer boreholes showed that the hydraulic conductivity further into the rock in general is below c. $1 \cdot 10^{-10}$ m/s. However, increased hydraulic conductivity was observed in section 10-14 m in the flowing borehole KXZSD8HL as estimated from inflow measurements. If KXZSD8HL is excluded, both the median and geometric mean of the estimated hydraulic conductivities of all tested sections (N=13) in the long boreholes are $K_M= K_{gm}= 3 \cdot 10^{-11}$ m/s. As before, this value is uncertain since several of the tests have conductivities below the practical lower measurement limit of the test system.

A potential water-conducting NW-fracture (147/62) was indicated from BIPS-measurements at 12.8 m in KXZSD8HL. The orientation of this fracture is in good agreement with the reported dominating orientation of fractures in the A-boreholes around the Zedex tunnel. The extrapolated fracture intersection in the Zedex tunnel at c. 65 m length is also in good agreement with an observed water-bearing fracture according to the structural model, see Appendix 5. Borehole radar measurements combined with tunnel mapping indicate two NW-fractures with similar orientation intersecting the Zedex tunnel at c. 72 m and c. 69 m length, respectively.

References

Carlsten, S.,1998: Zedex Project. High frequency radar antenna measurements in boreholes at the Zedex-tunnel. (In press).

Cooley, R., L., 1987: A method of estimating parameters and assessing reliability for models of steady state groundwater flow. 2. Application of statistical analysis. Water Resources Research, vol 21, no 10, pp 1525-1538.

Draper, N., R., Smith, H., 1982: Applied regression analysis, 2nd ed. New York: John Wiley and Sons.

Stenberg, L. and Gunnarsson D., 1998: Äspö Hard Rock Laboratory. Characterisation of the Zedex drift in advance of the Backfill and Plug Test. Progress Report HRL-98-10.

Stråhle, A., 1998: (pers.comm.)

Voss, C., I., 1990: SUTRA - A finite-element simulation model for saturated-unsaturated, fluid-density-dependent groundwater flow with energy transport or chemically-reactive single-species solute transport. Version V06902D. U.S: Geological Survey Water-Resources Investigations report 84-4369.

Table A1-1. Final borehole Test plan for single-packer hydraulic tests in the Zedex tunnel.

Rock instrum. Borehole	Length (m)	diameter (mm)	inclination ° + = up - =down
Test 24 holes	1	56	18 up, 6 down
KZ0041B02	5	56	-2
KZ0041G02	5	56	-90
KZ0041A02	5	56	2
KZ0065B02	5	56	-1
KZ0065G02	5	56	-90
KZ0065A02	5	56	-1
KXZSD8HR	23.16	86	-2 ?
KXZB3	15.2	56	-90 ?
KXZRD7H	8.2	86	-2 ?
KXZRD7HR	8.09	86	-2 ?
KXZA1	30.24	86	-1
KXZA2	35.14	56	-1.2
KXZA6	c. 40	56	-8.9

Table A1-2. Numbering and positions of instruments for measuring pore water pressure in the rock.

Type and number	Location	Measuring sect. (m)	Borehole	Diameter (mm)	Tested yes
UR1	Roof	0.5-1.0	KZ0065I01	56	
UR2	Roof	0.5-1.0	KZ0063I01	56	yes
UR3	Roof	0.5-1.0	KZ0061I01	56	
UR4	Roof	0.5-1.0	KZ0059I01	56	yes
UR5	Roof	0.5-1.0	KZ0057I01	56	
UR6	Roof	0.5-1.0	KZ0054I01	56	yes
UR7	Roof	0.5-1.0	KZ0052I01	56	
UR8	Roof	0.5-1.0	KZ0050I01	56	yes
UR9	Roof	0.5-1.0	KZ0048I01	56	
UR10	Roof	0.5-1.0	KZ0046I01	56	
UR11	Roof	0.5-1.0	KZ0043I01	56	
UR12	Roof	0.5-1.0	KZ0041I01	56	
UR21	Right wall	0.5-1.0	KZ0066B01	56	
UR22	Right wall	0.5-1.0	KZ0064B01	56	yes
UR23	Right wall	0.5-1.0	KZ0061B01	56	
UR24	Right wall	0.5-1.0	KZ0059B01	56	yes
UR25	Right wall	0.5-1.0	KZ0057B01	56	
UR26	Right wall	0.5-1.0	KZ0055B01	56	yes
UR27	Right wall	0.5-1.0	KZ0053B01	56	
UR28	Right wall	0.5-1.0	KZ0050B01	56	yes
UR29	Right wall	0.5-1.0	KZ0048B01	56	
UR30	Right wall	0.5-1.0	KZ0046B01	56	yes
UR31	Right wall	0.5-1.0	KZ0044B01	56	
UR32	Right wall	0.5-1.0	KZ0042B01	56	
UR41	Floor	0.5-1.0	KZ0065G01	56	
UR42	Floor	0.5-1.0	KZ0063G01	56	
UR43	Floor	0.5-1.0	KZ0061G01	56	yes
UR44	Floor	0.5-1.0	KZ0059G01	56	yes
UR45	Floor	0.5-1.0	KZ0057G01	56	yes
UR46	Floor	0.5-1.0	KZ0054G01	56	yes
UR47	Floor	0.5-1.0	KZ0052G01	56	yes
UR48	Floor	0.5-1.0	KZ0050G01	56	yes
UR49	Floor	0.5-1.0	KZ0048G01	56	yes
UR50	Floor	0.5-1.0	KZ0046G01	56	yes
UR51	Floor	0.5-1.0	KZ0043G01	56	yes
UR52	Floor	0.5-1.0	KZ0041G01	56	
UR61	Left wall	0.5-1.0	KZ0066A01	56	
UR62	Left wall	0.5-1.0	KZ0064A01	56	yes
UR63	Left wall	0.5-1.0	KZ0061A01	56	
UR64	Left wall	0.5-1.0	KZ0059A01	56	yes
UR65	Left wall	0.5-1.0	KZ0057A01	56	
UR66	Left wall	0.5-1.0	KZ0055A01	56	yes
UR67	Left wall	0.5-1.0	KZ0053A01	56	
UR68	Left wall	0.5-1.0	KZ0050A01	56	yes
UR69	Left wall	0.5-1.0	KZ0048A01	56	
UR70	Left wall	0.5-1.0	KZ0046A01	56	yes
UR71	Left wall	0.5-1.0	KZ0044A01	56	
UR72	Left wall	0.5-1.0	KZ0042A01	56	

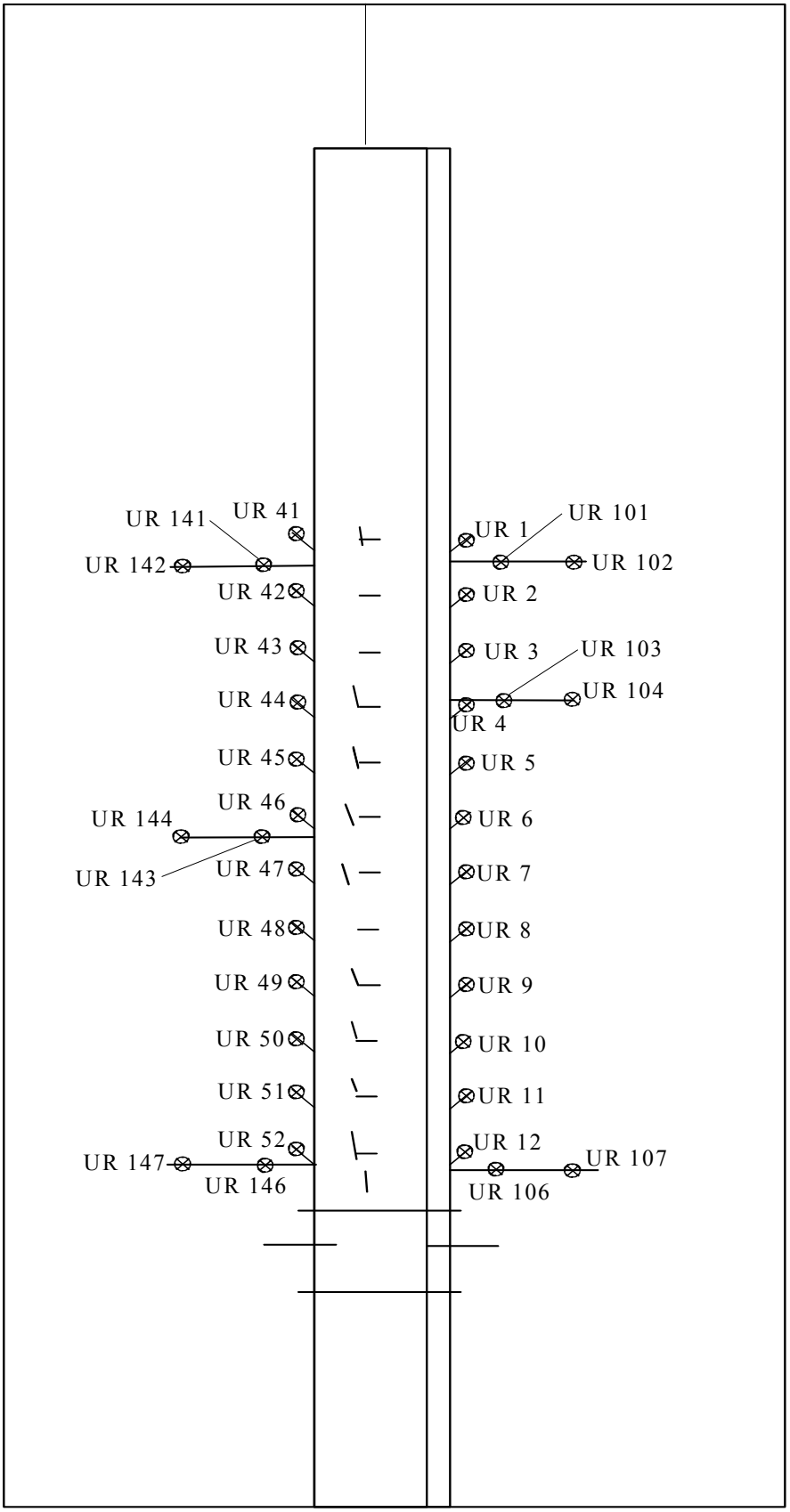

Fig A1-1. *Position of measuring points in the boreholes of the rock in the floor (left part) and the roof. Vertical section. (From Clay Technology).*

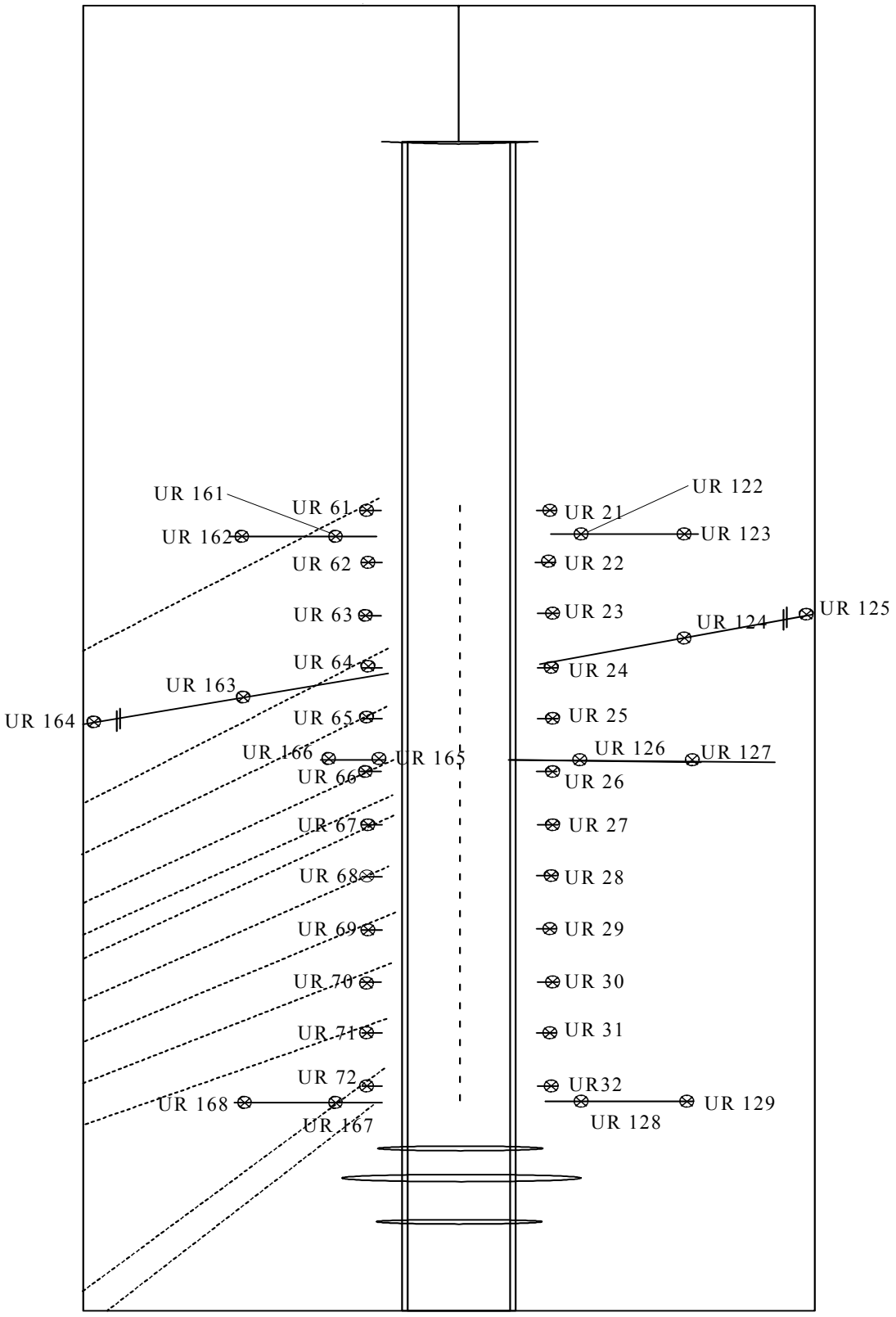

Figure A1-2. *Position of measuring points in the boreholes of the rock in the walls. Horizontal section. (From Clay Technology)*

Calibration chart between water level change (h mm) and volume V (ml). GEOSIGMA Flow meter.

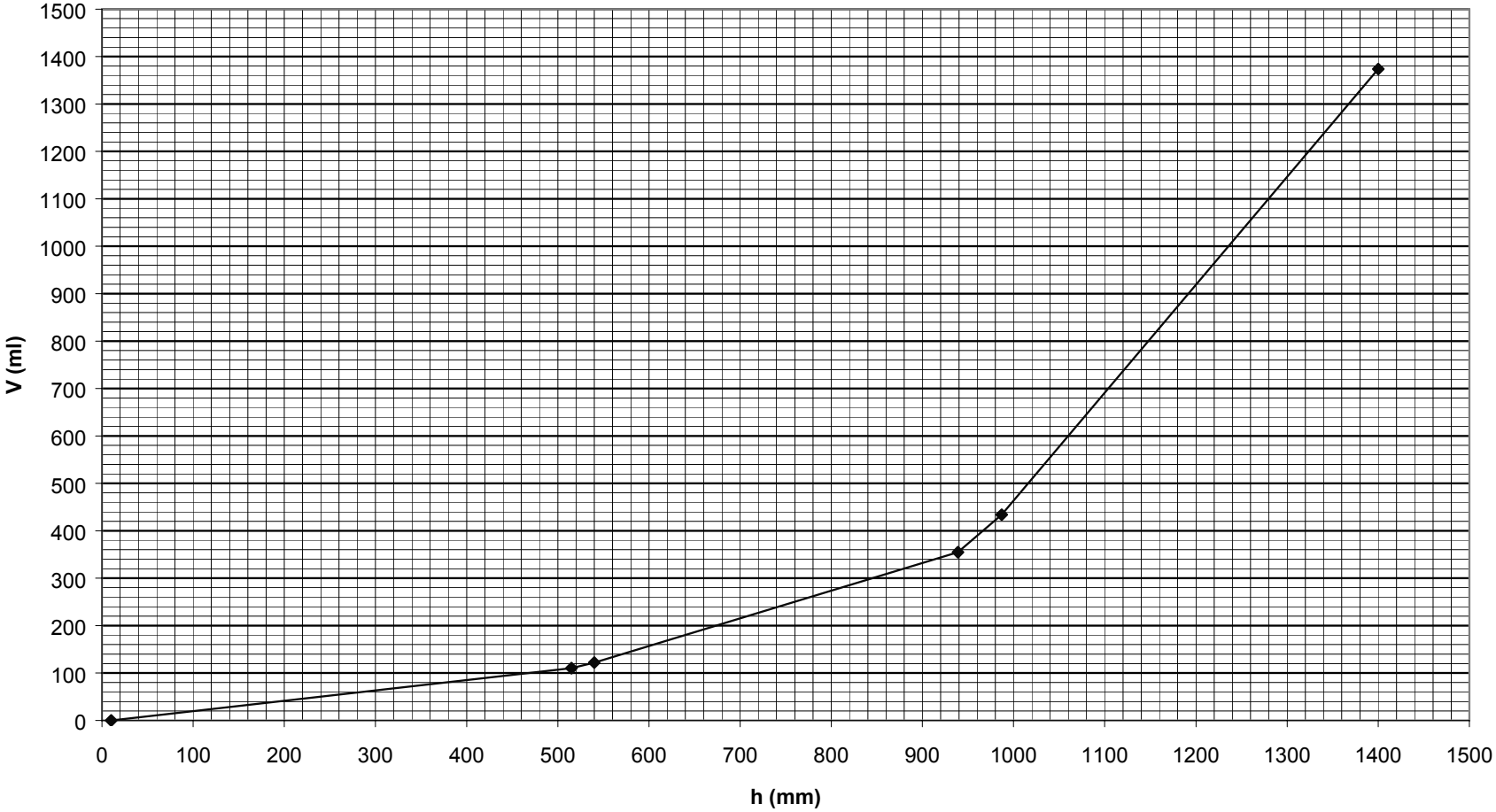

APPENDIX 2

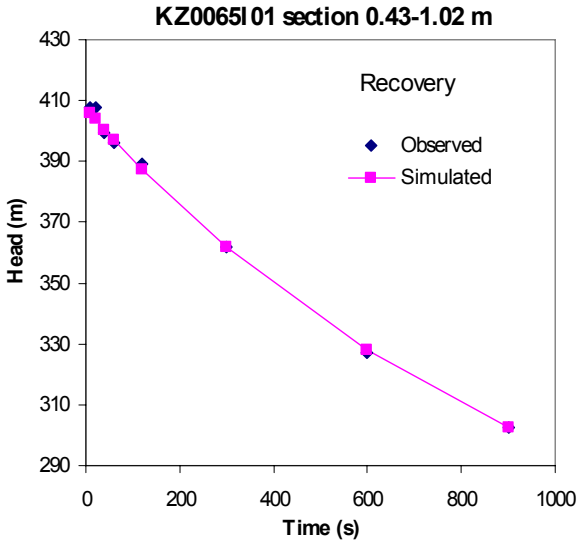
KZ0065I01 section 0.43-1.02 m
Recovery
Observed
Simulated
Head (m)
Time (s)
430
410
390
370
350
330
310
290
0
200
400
600
800
1000

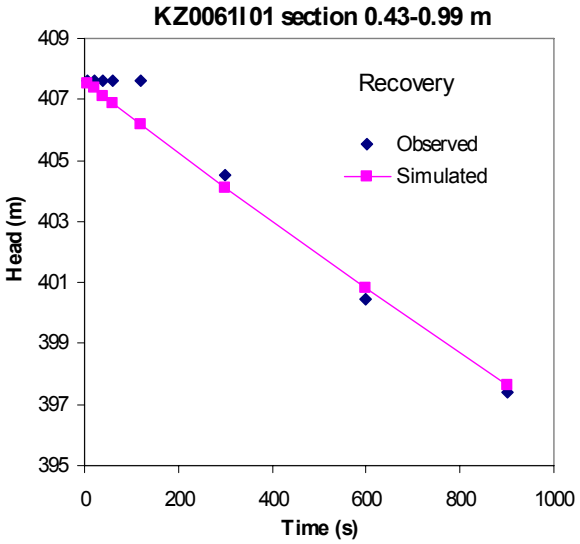
KZ0061I01 section 0.43-0.99 m
Recovery
Observed
Simulated
Head (m)
Time (s)
409
407
405
403
401
399
397
395
0
200
400
600
800
1000

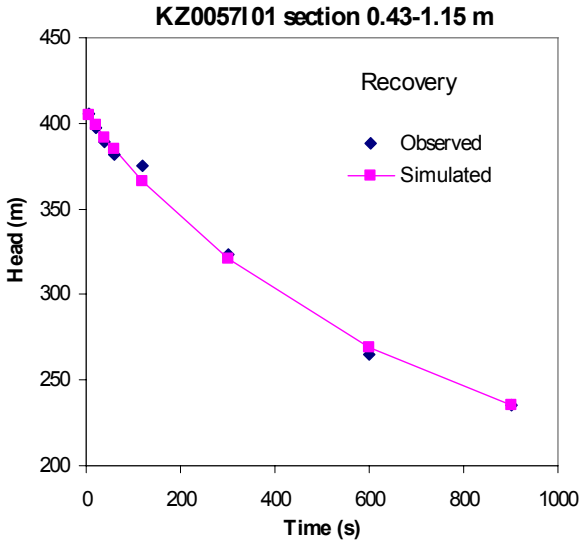
KZ0057I01 section 0.43-1.15 m
Recovery
Observed
Simulated
Head (m)
Time (s)
450
400
350
300
250
200
0
200
400
600
800
1000

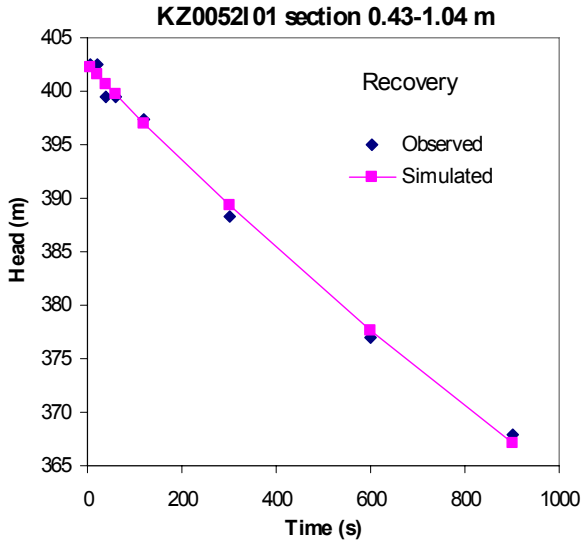
KZ0052I01 section 0.43-1.04 m
Recovery
Observed
Simulated
Head (m)
Time (s)
405
400
395
390
385
380
375
370
365
0
200
400
600
800
1000

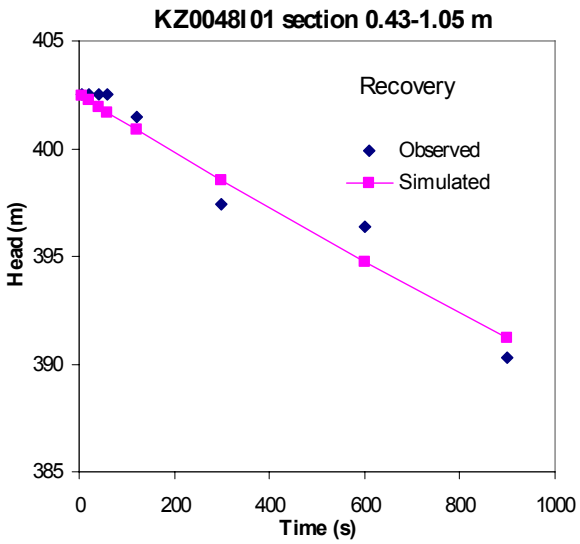
KZ0048I01 section 0.43-1.05 m
Recovery
Observed
Simulated
Head (m)
Time (s)
405
400
395
390
385
0
200
400
600
800
1000

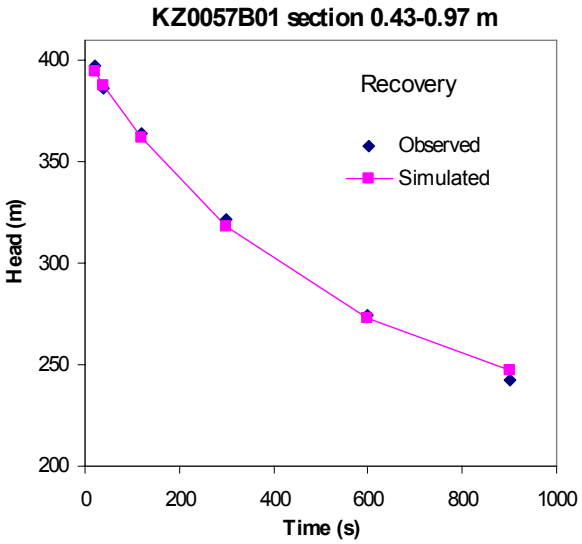
KZ0057B01 section 0.43-0.97 m
Recovery
Observed
Simulated
Head (m)
Time (s)
400
350
300
250
200
0
200
400
600
800
1000

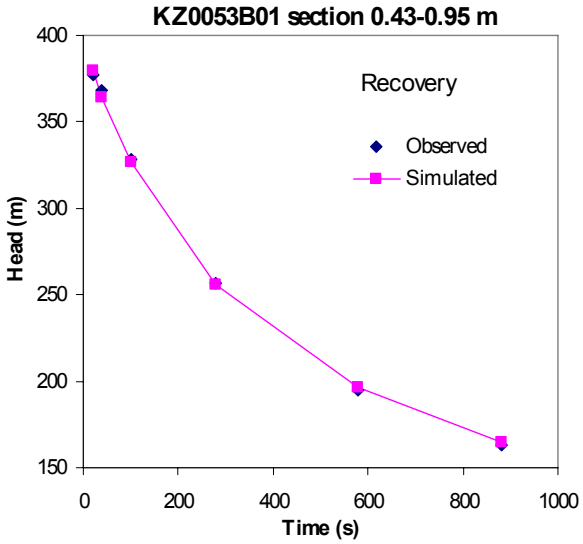
KZ0053B01 section 0.43-0.95 m
Recovery
Observed
Simulated
Head (m)
Time (s)
400
350
300
250
200
150
0
200
400
600
800
1000

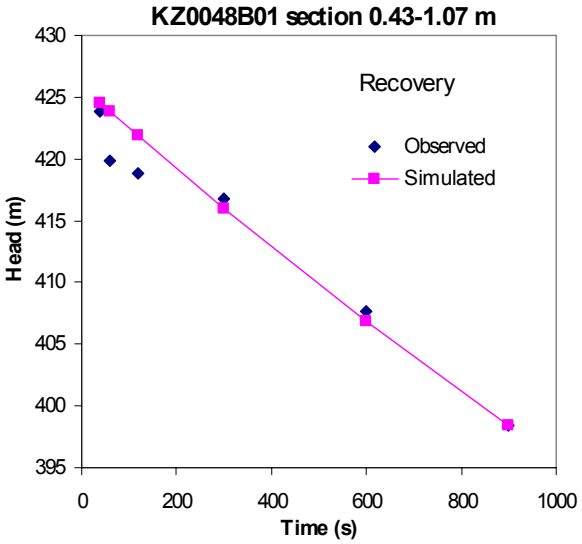
KZ0048B01 section 0.43-1.07 m
Recovery
Observed
Simulated
Head (m)
Time (s)
430
425
420
415
410
405
400
395
0
200
400
600
800
1000

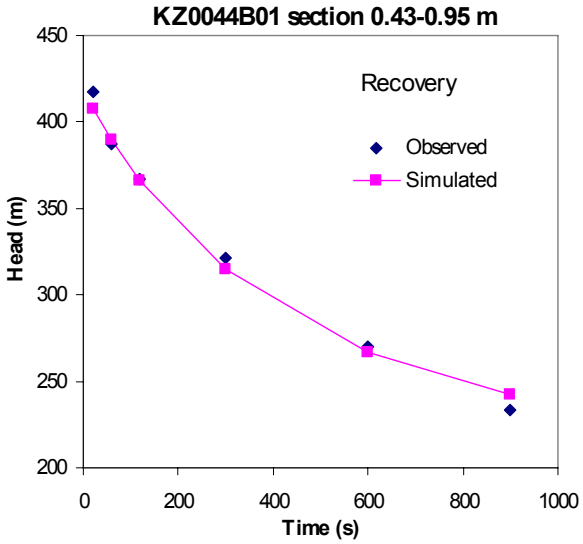
KZ0044B01 section 0.43-0.95 m
Recovery
Observed
Simulated
Head (m)
Time (s)
450
400
350
300
250
200
0
200
400
600
800
1000

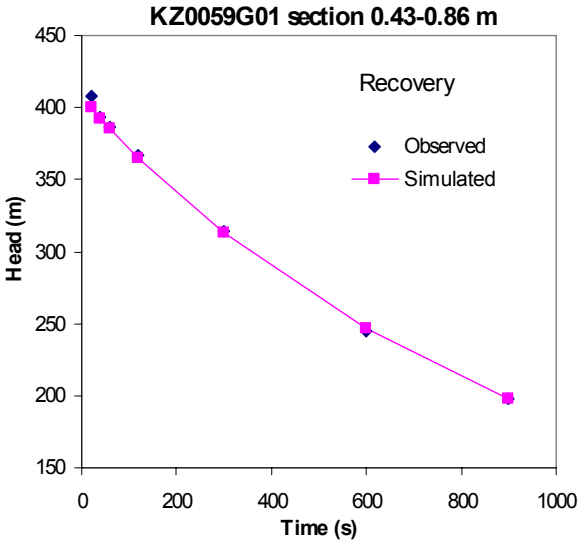
KZ0059G01 section 0.43-0.86 m
Recovery
Observed
Simulated
Head (m)
Time (s)
450
400
350
300
250
200
150
0
200
400
600
800
1000

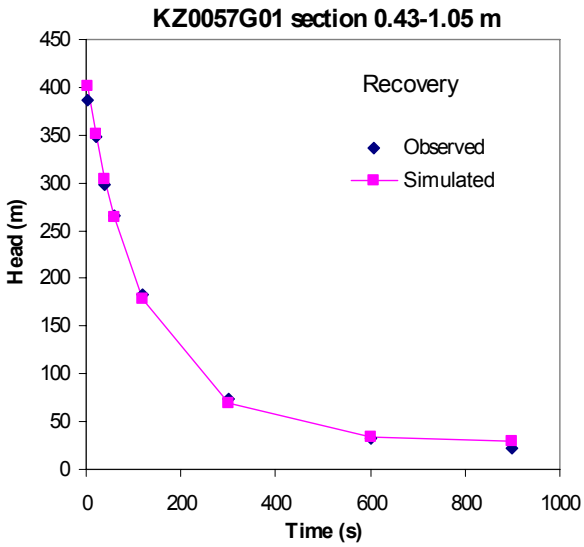
KZ0057G01 section 0.43-1.05 m
Recovery
Observed
Simulated
Head (m)
Time (s)
450
400
350
300
250
200
150
100
50
0
0
200
400
600
800
1000

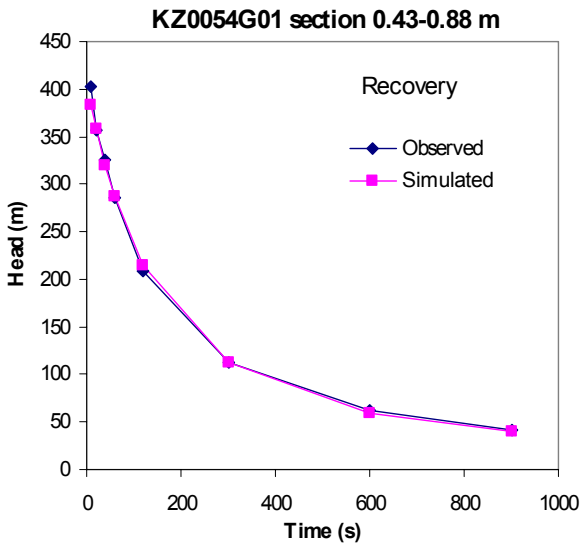
KZ0054G01 section 0.43-0.88 m
Recovery
Observed
Simulated
Head (m)
Time (s)
450
400
350
300
250
200
150
100
50
0
0
200
400
600
800
1000

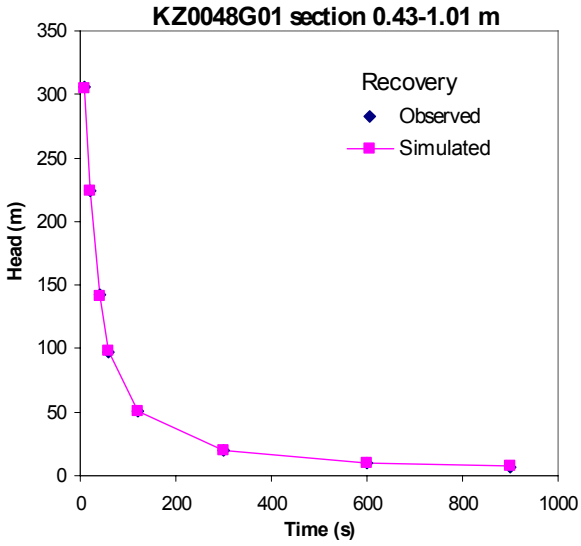
KZ0048G01 section 0.43-1.01 m
Recovery
Observed
Simulated
Head (m)
Time (s)
350
300
250
200
150
100
50
0
0
200
400
600
800
1000

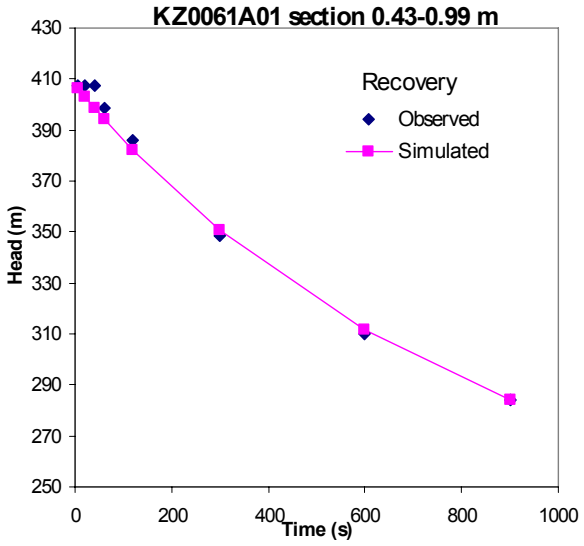
KZ0061A01 section 0.43-0.99 m
Recovery
Observed
Simulated
Head (m)
Time (s)
430
410
390
370
350
330
310
290
270
250
0
200
400
600
800
1000

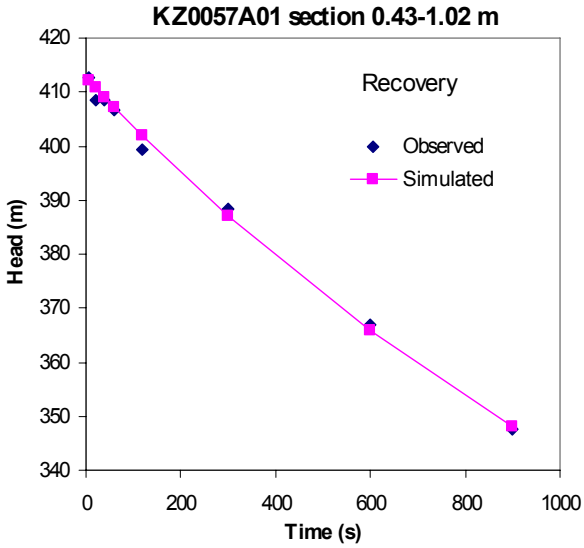
KZ0057A01 section 0.43-1.02 m
Recovery
Observed
Simulated
Head (m)
Time (s)
420
410
400
390
380
370
360
350
340
0
200
400
600
800
1000

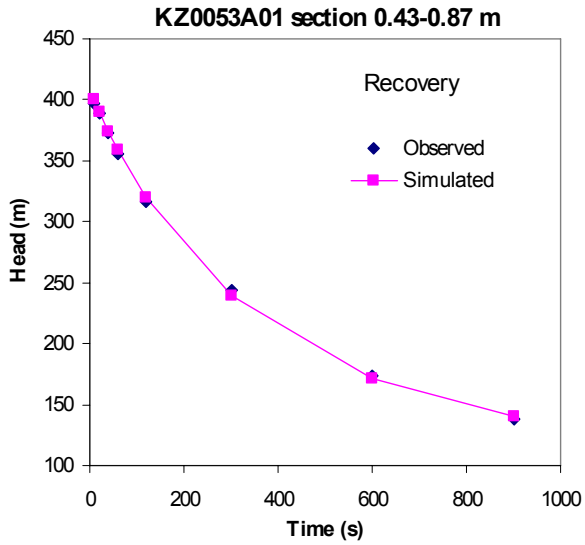
KZ0053A01 section 0.43-0.87 m
Recovery
Observed
Simulated
Head (m)
Time (s)
450
400
350
300
250
200
150
100
0
200
400
600
800
1000

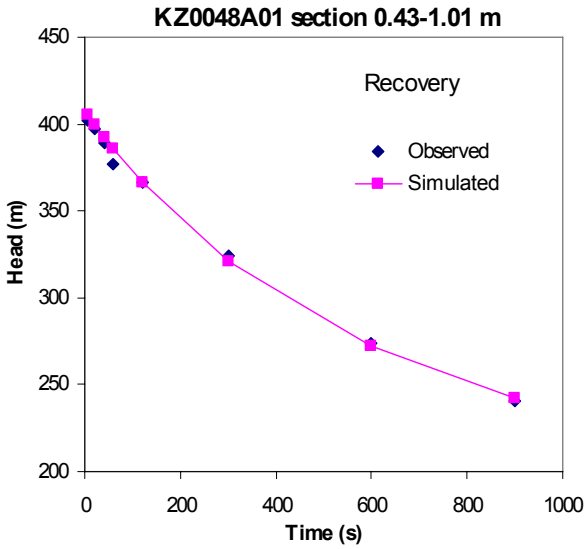
KZ0048A01 section 0.43-1.01 m
Recovery
Observed
Simulated
Head (m)
Time (s)
450
400
350
300
250
200
0
200
400
600
800
1000

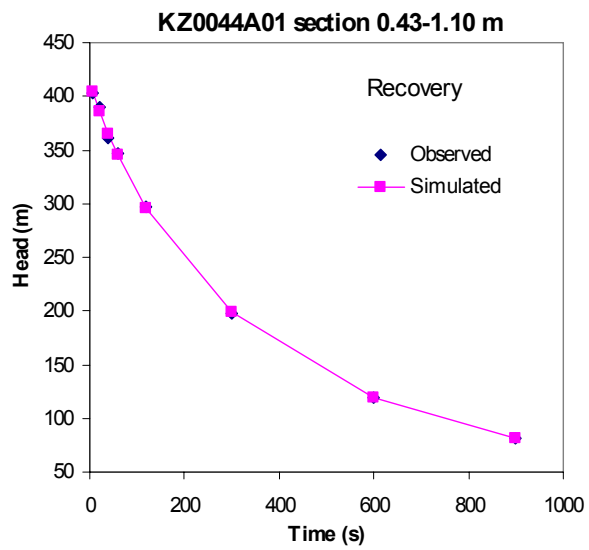
KZ0044A01 section 0.43-1.10 m
Recovery
Observed
Simulated
Head (m)
Time (s)
450
400
350
300
250
200
150
100
50
0
200
400
600
800
1000

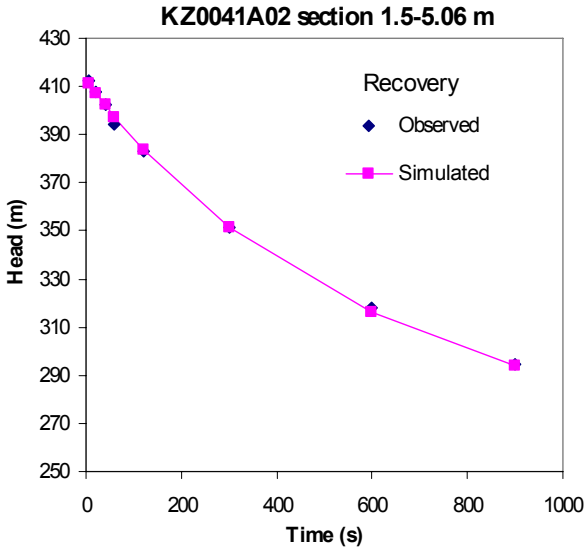
KZ0041A02 section 1.5-5.06 m
Recovery
Observed
Simulated
Head (m)
Time (s)
430
410
390
370
350
330
310
290
270
250
0
200
400
600
800
1000

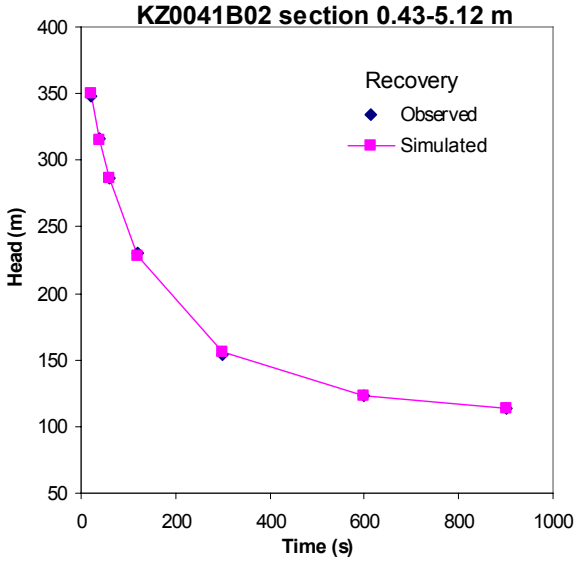
KZ0041B02 section 0.43-5.12 m
Recovery
Observed
Simulated
Head (m)
Time (s)
400
350
300
250
200
150
100
50
0
200
400
600
800
1000

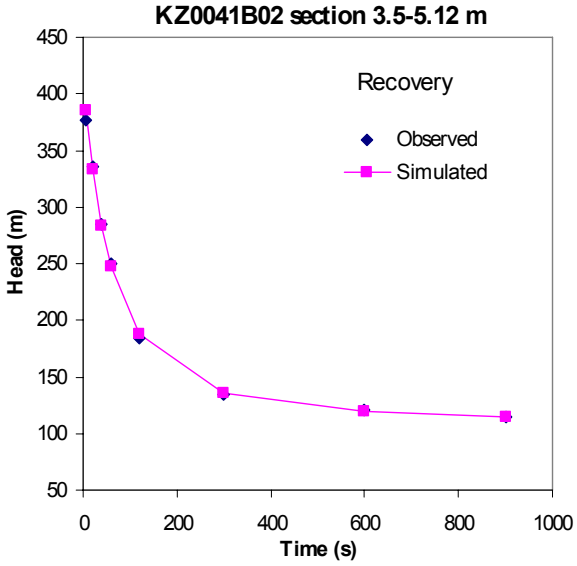
KZ0041B02 section 3.5-5.12 m
Recovery
Observed
Simulated
Head (m)
Time (s)
450
400
350
300
250
200
150
100
50
0
200
400
600
800
1000

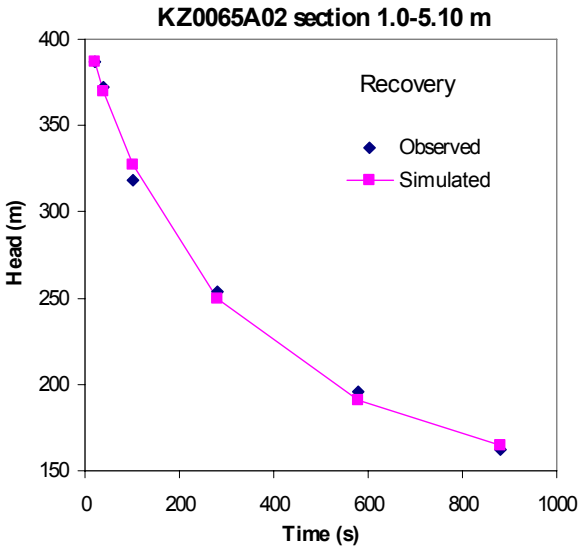
KZ0065A02 section 1.0-5.10 m
Recovery
Observed
Simulated
Head (m)
Time (s)
400
350
300
250
200
150
0
200
400
600
800
1000

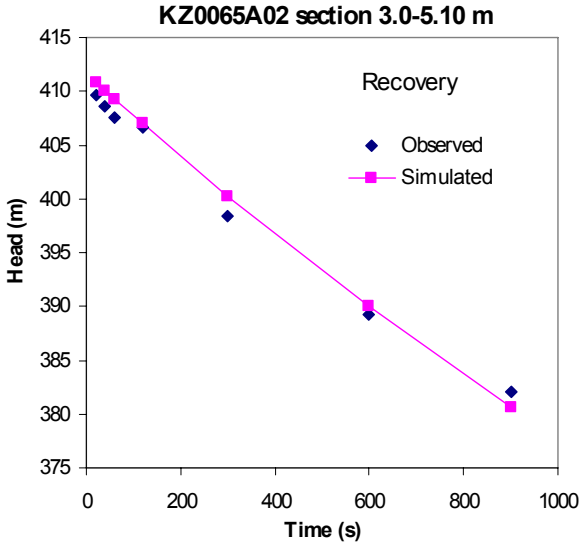
KZ0065A02 section 3.0-5.10 m
Recovery
Observed
Simulated
Head (m)
Time (s)
415
410
405
400
395
390
385
380
375
0
200
400
600
800
1000

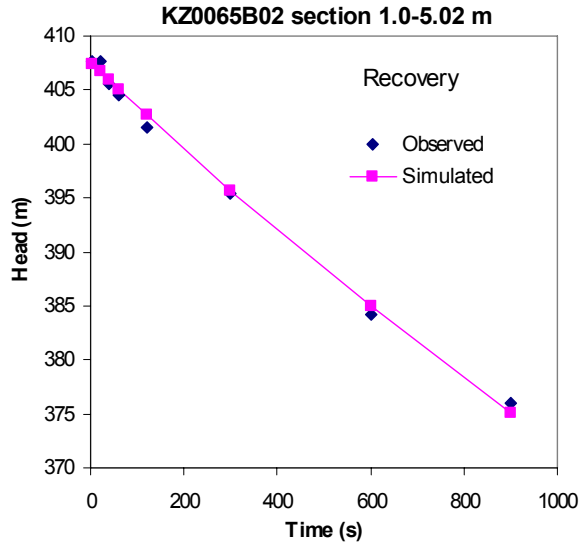
KZ0065B02 section 1.0-5.02 m
Recovery
Observed
Simulated
Head (m)
Time (s)
410
405
400
395
390
385
380
375
370
0
200
400
600
800
1000

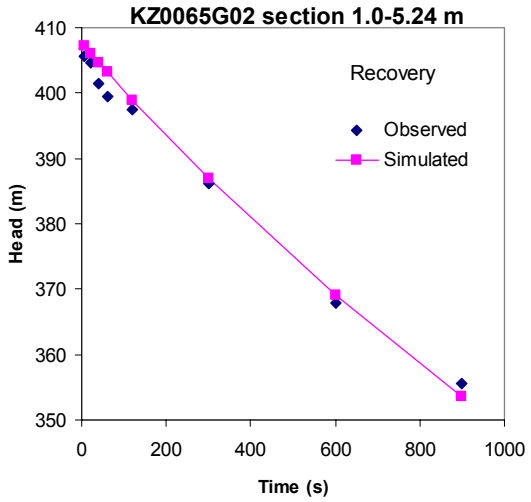
KZ0065G02 section 1.0-5.24 m
Recovery
Observed
Simulated
Head (m)
Time (s)
410
400
390
380
370
360
350
0
200
400
600
800
1000

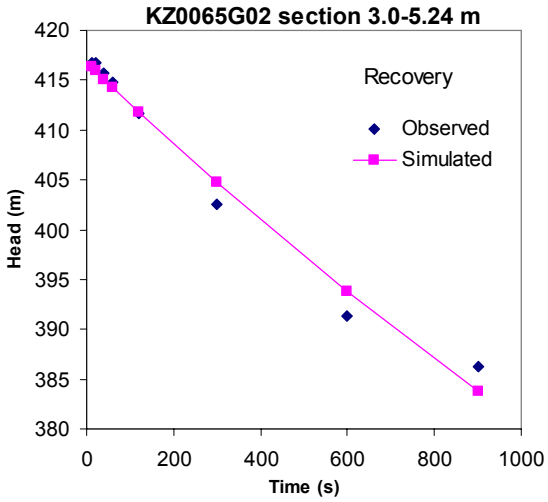
KZ0065G02 section 3.0-5.24 m
Recovery
Observed
Simulated
Head (m)
Time (s)
420
415
410
405
400
395
390
385
380
0
200
400
600
800
1000

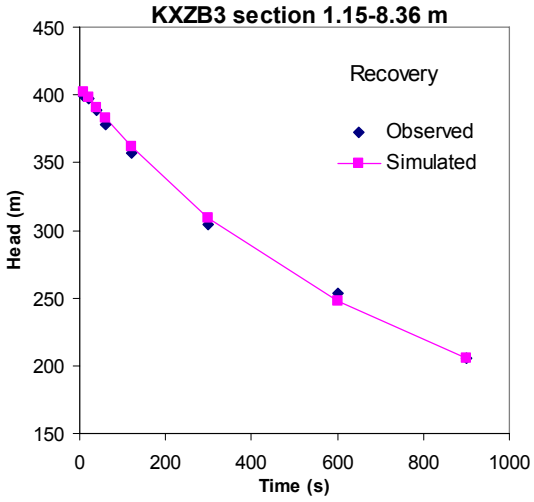
KXZB3 section 1.15-8.36 m
Recovery
Observed
Simulated
Head (m)
Time (s)
450
400
350
300
250
200
150
0
200
400
600
800
1000

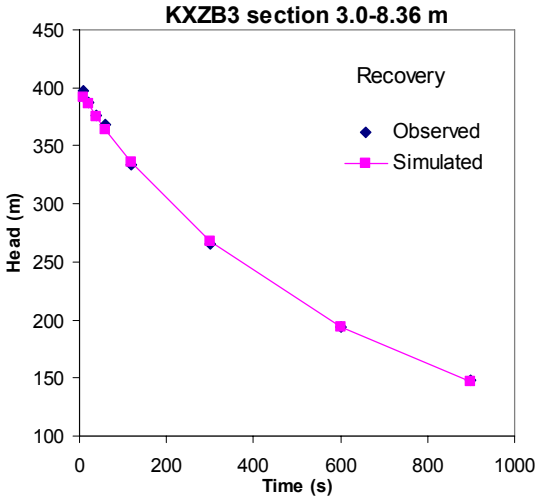
KXZB3 section 3.0-8.36 m
Recovery
Observed
Simulated
Head (m)
Time (s)
450
400
350
300
250
200
150
100
0
200
400
600
800
1000

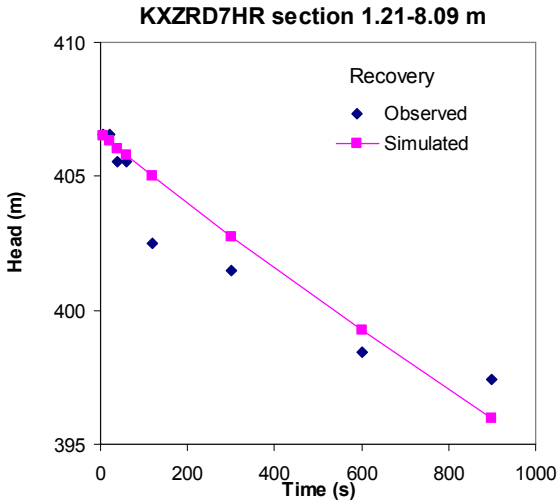
KXZRD7HR section 1.21-8.09 m
Recovery
Observed
Simulated
Head (m)
Time (s)
410
405
400
395
0
200
400
600
800
1000

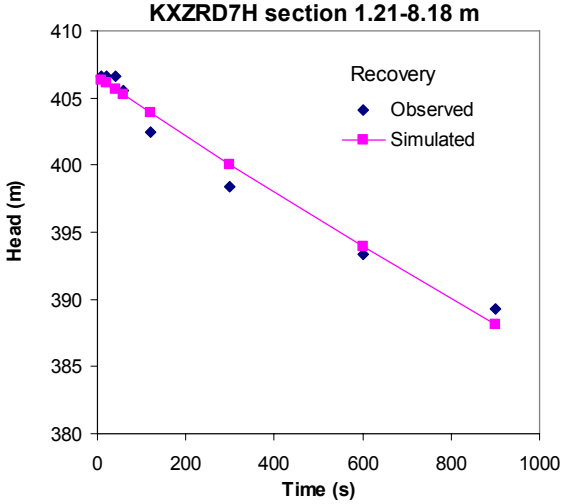
KXZRD7H section 1.21-8.18 m
Recovery
Observed
Simulated
Head (m)
Time (s)
410
405
400
395
390
385
380
0
200
400
600
800
1000

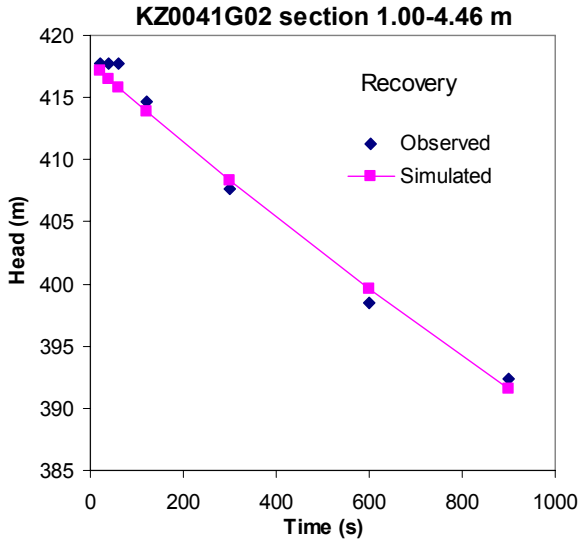
KZ0041G02 section 1.00-4.46 m
Recovery
Observed
Simulated
Head (m)
Time (s)
420
415
410
405
400
395
390
385
0
200
400
600
800
1000

Table A4-1a. Results from the injection phase of the tests in the 1 m-boreholes.

BOREHOLE SECTION			INJECTION PHASE				
Borehole	**Length (m)**	**Measured Section (m)**	**Flow rate Q_p (ml/min)**	**Pressure P_p (bar)**	**T_{ss}($m^{2/s}$)**	**K_{ss} (m/s)**	**Comments**
KZ0065I01 (UR1)	1.02	0.43-1.02	0.5	40	$5.3 \cdot 10^{-11}$	$9.0 \cdot 10^{-11}$	
KZ0061I01 (UR3)	0.99	0.43-0.99	0.2	40	$2.1 \cdot 10^{-11}$	$3.8 \cdot 10^{-11}$	
KZ0057I01 (UR5)	1.15	0.43-1.15	0.8	39.9	$8.5 \cdot 10^{-11}$	$1.2 \cdot 10^{-10}$	
KZ0052I01 (UR7)	1.04	0.43-1.04	0.2	39.5	$2.2 \cdot 10^{-11}$	$3.6 \cdot 10^{-11}$	
KZ0048I01 (UR9)	1.05	0.43-1.05	0.1	39.5	$1.1 \cdot 10^{-11}$	$1.8 \cdot 10^{-11}$	
KZ0061B01 (UR23)	0.95	0.43 - 0.95	220	38.1	$\geq 2.7 \cdot 10^{-8}$	$\geq 5.1 \cdot 10^{-8}$	Rock leakage
KZ0057B01 (UR25)	0.97	0.43 - 0.97	1.0	39.5	$1.1 \cdot 10^{-10}$	$2.0 \cdot 10^{-10}$	
KZ0053B01 (UR27)	0.95	0.43 - 0.95	2.0	38.9	$2.3 \cdot 10^{-10}$	$4.4 \cdot 10^{-10}$	
KZ0048B01 (UR29)	1.07	0.43 – 1.07	0.09	41.8	$8.4 \cdot 10^{-12}$	$1.3 \cdot 10^{-11}$	
KZ0044B01 (UR31)	0.95	0.43 - 0.95	0.9	41	$8.9 \cdot 10^{-11}$	$1.7 \cdot 10^{-10}$	
KZ0059G01 (UR44)	0.86	0.43 - 0.86	1.4	40	$1.5 \cdot 10^{-10}$	$3.4 \cdot 10^{-10}$	
KZ0057G01 (UR45)	1.05	0.43 – 1.05	6.2	39.9	$6.6 \cdot 10^{-10}$	$1.1 \cdot 10^{-9}$	
KZ0054G01 (UR46)	0.88	0.43 - 0.88	3.8	39.9	$4.0 \cdot 10^{-10}$	$8.9 \cdot 10^{-10}$	
KZ0052G01 (UR47)	(0.1)	-	-	-	-	-	Borh. grouted
KZ0050G01 (UR48)	1	-	-	-	$>5 \cdot 10^{-8}$	$>1 \cdot 10^{-7}$	Int. fract. rock
KZ0048G01 (UR49)	1.01	0.43 – 1.01	22.4	39.9	$2.4 \cdot 10^{-9}$	$4.1 \cdot 10^{-9}$	(Rock leakage)
KZ0046G01 (UR50)	1	-	-	-	$>5 \cdot 10^{-8}$	$>1 \cdot 10^{-7}$	Rock leakage
KZ0043G01 (UR51)	0.95	-	-	-	$>5 \cdot 10^{-8}$	$>1 \cdot 10^{-7}$	Rock leakage
KZ0041G01 (UR52)	0.96	-	-	-	$>5 \cdot 10^{-8}$	$>1 \cdot 10^{-7}$	Rock leakage
KZ0061A01 (UR63)	0.99	0.43 - 0.99	0.7	40.9	$7.0 \cdot 10^{-11}$	$1.3 \cdot 10^{-10}$	
KZ0057A01 (UR65)	1.02	0.43 – 1.02	1.0	40.5	$9.9 \cdot 10^{-11}$	$1.7 \cdot 10^{-10}$	
KZ0053A01 (UR67)	0.87	0.43 - 0.87	2.2	40	$2.3 \cdot 10^{-10}$	$5.2 \cdot 10^{-10}$	
KZ0048A01 (UR69)	1.01	0.43 – 1.01	0.9	40	$9.5 \cdot 10^{-11}$	$1.6 \cdot 10^{-10}$	
KZ0044A01 (UR71)	1.10	0.43 – 1.10	2.0	40.3	$2.0 \cdot 10^{-10}$	$3.0 \cdot 10^{-10}$	

Table A4-1b. Results from the recovery phase of the tests in the 1 m-boreholes.

BOREHOLE SECTION			RECOVERY PHASE				
Borehole	**Length (m)**	**Measured Section (m)**	**Log T_R (log m^2/s)**	**SE_{LogTR} log ($m^{2/s}$)**	**T_R (m^2/s)**	**K_R (m/s)**	**Comments**
KZ0065I01 (UR1)	1.02	0.43-1.02	-9.58	0.23	$2.6 \cdot 10^{-10}$	$4.5 \cdot 10^{-10}$	
KZ0061I01 (UR3)	0.99	0.43-0.99	-10.41	7.57	$3.9 \cdot 10^{-11}$	$6.9 \cdot 10^{-11}$	
KZ0057I01 (UR5)	1.15	0.43-1.15	-9.42	0.32	$3.8 \cdot 10^{-10}$	$5.3 \cdot 10^{-10}$	
KZ0052I01 (UR7)	1.04	0.43-1.04	-10.35	0.11	$4.5 \cdot 10^{-11}$	$7.3 \cdot 10^{-11}$	
KZ0048I01 (UR9)	1.05	0.43-1.05	-11.02	9.2	$9.6 \cdot 10^{-12}$	$1.5 \cdot 10^{-11}$	
KZ0061B01 (UR23)	0.95	0.43 - 0.95	-	-	-	-	Rock leakage
KZ0057B01 (UR25)	0.97	0.43 - 0.97	-9.62	0.11	$2.4 \cdot 10^{-10}$	$4.4 \cdot 10^{-10}$	
KZ0053B01 (UR27)	0.95	0.43 - 0.95	-9.65	0.61	$2.2 \cdot 10^{-10}$	$4.3 \cdot 10^{-10}$	
KZ0048B01 (UR29)	1.07	0.43 – 1.07	-10.75	20.5	$1.8 \cdot 10^{-11}$	$2.8 \cdot 10^{-11}$	
KZ0044B01 (UR31)	0.95	0.43 - 0.95	-9.67	0.17	$2.1 \cdot 10^{-10}$	$4.1 \cdot 10^{-10}$	
KZ0059G01 (UR44)	0.86	0.43 - 0.86	-9.91	0.14	$1.2 \cdot 10^{-10}$	$2.9 \cdot 10^{-10}$	
KZ0057G01 (UR45)	1.05	0.43 – 1.05	-9.79	0.19	$1.6 \cdot 10^{-10}$	$2.6 \cdot 10^{-10}$	
KZ0054G01 (UR46)	0.88	0.43 - 0.88	-9.17	0.04	$6.8 \cdot 10^{-10}$	$1.5 \cdot 10^{-9}$	
KZ0052G01 (UR47)	(0.1)	-	-	-	-	-	Boreh. grouted
KZ0050G01 (UR48)	1	-	-	-	-	-	Intens.frac. rock
KZ0048G01 (UR49)	1.01	0.43 – 1.01	-8.22	0.003	$6.0 \cdot 10^{-9}$	$1.0 \cdot 10^{-8}$	(Rock leakage)
KZ0046G01 (UR50)	1	-	-	-	-	-	Rock leakage
KZ0043G01 (UR51)	0.95	-	-	-	-	-	Rock leakage
KZ0041G01 (UR52)	0.96	-	-	-	-	-	Rock leakage
KZ0061A01 (UR63)	0.99	0.43 - 0.99	-9.49	0.40	$3.2 \cdot 10^{-10}$	$5.8 \cdot 10^{-10}$	
KZ0057A01 (UR65)	1.02	0.43 – 1.02	-10.07	0.53	$8.5 \cdot 10^{-11}$	$1.4 \cdot 10^{-10}$	
KZ0053A01 (UR67)	0.87	0.43 - 0.87	-10.23	0.03	$5.9 \cdot 10^{-11}$	$1.3 \cdot 10^{-10}$	
KZ0048A01 (UR69)	1.01	0.43 – 1.01	-9.75	0.15	$1.8 \cdot 10^{-10}$	$3.1 \cdot 10^{-10}$	
KZ0044A01 (UR71)	1.10	0.43 – 1.10	-9.61	0.01	$2.5 \cdot 10^{-10}$	$3.7 \cdot 10^{-10}$	

Table A4-2a. Results from the injection phase of the tests in the 5 m- and 8 m-boreholes and from the inflow tests in KXZSD8HL.

BOREHOLE SECTION			INJECTION PHASE				
Borehole	**Length (m)**	**Measured Section (m)**	**Flow rate Q_p (ml/min)**	**Pressure P_p (bar)**	**T_{ss}($m^{2/s}$)**	**K_{ss} ((m/s)**	**Comments**
KZ0041A02-1	5.06	1.5 – 5.06	1.6	40.5	$1.6 \cdot 10^{-10}$	$4.6 \cdot 10^{-11}$	
KZ0041B02-1	5.12	1.5 – 5.12	13.1	38.8	$1.5 \cdot 10^{-9}$	$4.1 \cdot 10^{-10}$	
KZ0041B02-2		3.5 – 5.12	11.6	39.9	$1.2 \cdot 10^{-9}$	$7.6 \cdot 10^{-10}$	
KZ0041G02-1	4.46	1.0 - 4.46-	0.3	41	$2.6 \cdot 10^{-11}$	$7.5 \cdot 10^{-12}$	
KZ0065A02-1	5.10	1.0 – 5.10	11	40	$1.2 \cdot 10^{-9}$	$2.8 \cdot 10^{-10}$	
KZ0065A02-2		3.0– 5.10	1.1	40.4	$1.1 \cdot 10^{-10}$	$5.2 \cdot 10^{-11}$	
KZ0065B02-1	5.02	1.0 – 5.02	0.7	40	$6.9 \cdot 10^{-11}$	$1.7 \cdot 10^{-11}$	
KZ0065G02-1	5.24	1.0 – 5.24	1.1	40	$1.2 \cdot 10^{-10}$	$2.8 \cdot 10^{-11}$	
KZ0065G02-2		3.0– 5.24	0.1	40.9	$9.5 \cdot 10^{-12}$	$4.2 \cdot 10^{-12}$	
KXZB3-1	8.36	1.15 – 8.36	2.4	39.9	$2.6 \cdot 10^{-10}$	$3.5 \cdot 10^{-11}$	
KXZB3-2		3.0 – 8.36	3.6	39.1	$4.0 \cdot 10^{-10}$	$7.5 \cdot 10^{-11}$	
KXZRD7HR	8.09	1.21 – 8.09	0.1	39.9	$1.1 \cdot 10^{-11}$	$1.5 \cdot 10^{-12}$	
KXZRD7H	8.18	1.21 – 8.18	0.8	39.9	$8.5 \cdot 10^{-11}$	$1.2 \cdot 10^{-11}$	
KXZSD8HR	23.16						Not tested
KXZSD8HL	25.98		c. 900				Main inflow localized at 10-14 m

Table A4-2b. Results from the recovery phase of the tests in the 5 m- and 8 m-boreholes.

BOREHOLE SECTION			INJECTION PHASE				
Borehole	**Length (m)**	**Measured Section (m)**	**Log T_R (log m^2/s)**	**SE_{LogTR} log ($m^{2/s}$)**	**T_R (m^2/s)**	**K_R (m/s)**	**Comments**
KZ0041A02-1	5.06	1.5 – 5.06	-9.43	0.02	$3.7 \cdot 10^{-10}$	$1.0 \cdot 10^{-10}$	
KZ0041B02-1	5.12	1.5 – 5.12	-8.68	0.04	$2.1 \cdot 10^{-9}$	$5.8 \cdot 10^{-10}$	
KZ0041B02-2		3.5 – 5.12	-8.42	0.08	$3.8 \cdot 10^{-9}$	$2.3 \cdot 10^{-9}$	
KZ0041G02-1	4.46	1.0 – 4.46	-10.07	11.4	$8.5 \cdot 10^{-11}$	$2.5 \cdot 10^{-11}$	
KZ0065A02-1	5.10	1.0 – 5.10	-9.45	0.20	$3.5 \cdot 10^{-10}$	$8.7 \cdot 10^{-11}$	
KZ0065A02-2		3.0– 5.10	-10.69	2.5	$2.0 \cdot 10^{-11}$	$9.7 \cdot 10^{-12}$	
KZ0065B02-1	5.02	1.0 – 5.02	-10.28	1.4	$5.2 \cdot 10^{-11}$	$1.3 \cdot 10^{-11}$	
KZ0065G02-1	5.24	1.0 – 5.24	-9.65	1.4	$2.2 \cdot 10^{-10}$	$5.3 \cdot 10^{-11}$	
KZ0065G02-2		3.0– 5.24	-10.81	2.34	$1.5 \cdot 10^{-11}$	$6.9 \cdot 10^{-12}$	
KXZB3-1	8.36	1.15 – 8.36	-9.84	0.27	$1.4 \cdot 10^{-10}$	$2.0 \cdot 10^{-11}$	
KXZB3-2		3.0 – 8.36	-9.63	0.04	$2.3 \cdot 10^{-10}$	$4.4 \cdot 10^{-11}$	
KXZRD7HR	8.09	1.21 – 8.09	-10.40	6.18	$4.0 \cdot 10^{-11}$	$5.8 \cdot 10^{-12}$	
KXZRD7H	8.18	1.21 – 8.18	-11.19	2.74	$6.5 \cdot 10^{-12}$	$9.3 \cdot 10^{-13}$	
KXZSD8HR	23.16	-	-	-	-	-	Not tested

ZEDEX TUNNEL

Structural model (Stenberg and Gunnarsson, 1998)

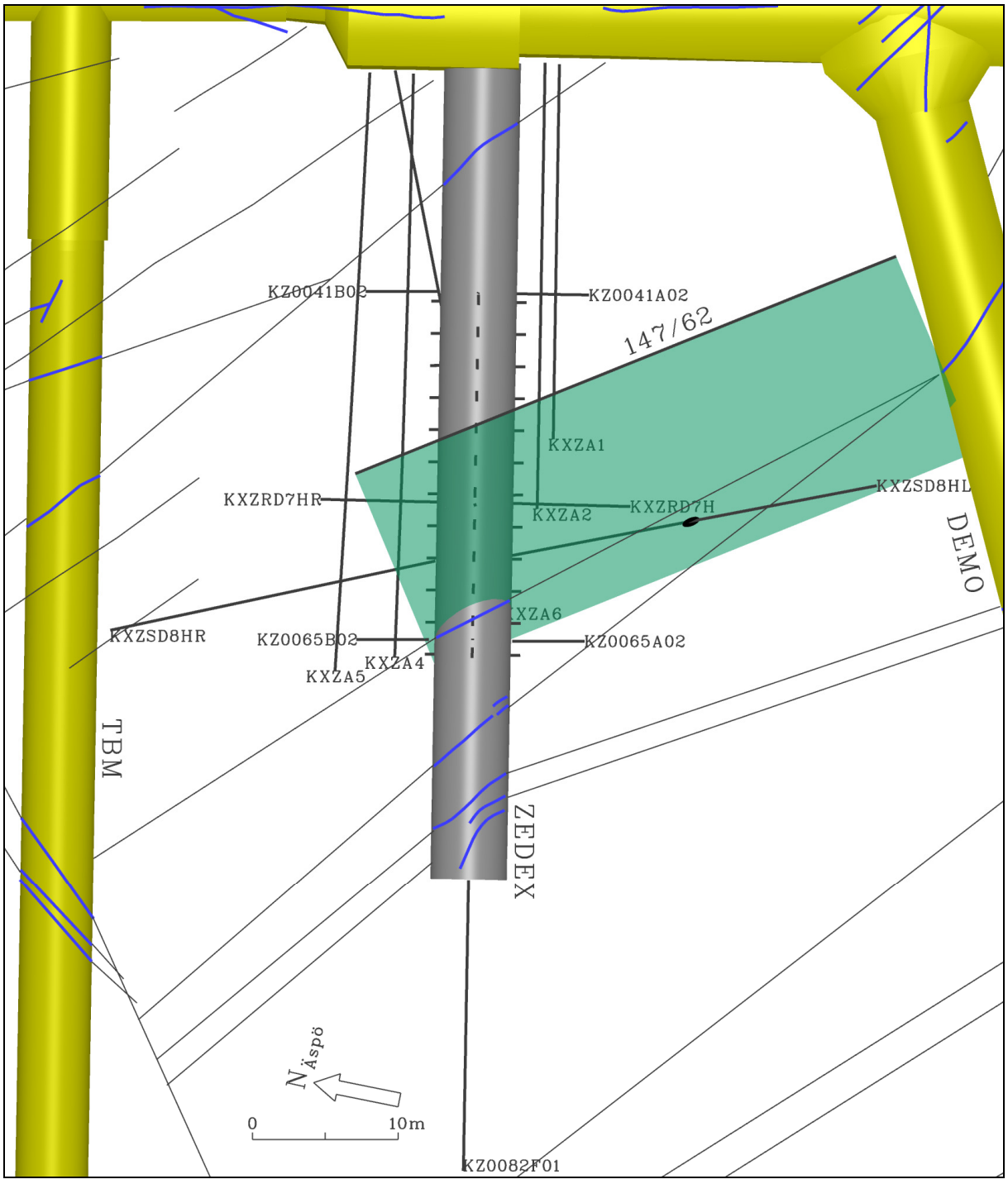

GEOSIGMA AB

Waterbearing fracture

Proposed interconnection between observed waterbearing fractures

Possible extrapolation of waterbearing fracture in KXZSD8HL